Marine and Petroleum Geology 150 (2023) 106153

Contents lists available at ScienceDirect

Marine and Petroleum Geology

journal homepage: www.elsevier.com/locate/marpetgeo

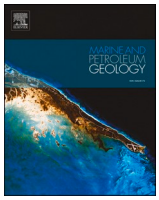

Paleoenvironmental and diagenetic evolution of the Aptian Pre-Salt succession in Namibe Basin (Onshore Angola)

Mar Moragas [a,b,*], Vinyet Baqués [a], Juan Diego Martín-Martín [c], Ian Sharp [d], Fabio Lapponi [d], David Hunt [d], Michael Zeller [d], Jaume Vergés [a,**], Grégoire Messager [d], Laurent Gindre-Chanu [d], Roger Swart [e], Vladimir Machado [f]

[a] Geosciences Barcelona (GEO3BCN-CSIC), Lluís Solé i Sabarís s/n, Barcelona, 08028, Spain
[b] Department of Earth Sciences, University of Bergen, Bergen, Norway
[c] Departament de Mineralogia, Petrologia i Geologia Aplicada, Facultat de Ciències de la Terra, Universitat de Barcelona (UB), c/Martí i Franquès s/n, Barcelona, 08028, Spain
[d] Equinor ASA, Norway, Sandsliveien 90, Sandsli, Bergen, Norway
[e] BlackGold Geosciences cc, P.O. Box 24287, Windhoek, Namibia
[f] Centro de Pesquisa e Desenvolvimento da Sonangol (Sonangol Research and Development Center), Rua Rainha Ginga n. 29/31, C.P. 1316, Luanda, Angola

ARTICLE INFO

Keywords:
Pre-salt
Onshore Angola
Namibe basin
Diagenesis
Sedimentology
Palaeovalley

ABSTRACT

The Aptian Pre-Salt sedimentary succession cropping out in Cangulo palaeovalley onshore Namibe Basin (Angola) was studied by a combination of field and analytical techniques to constrain the sedimentary and diagenetic evolution of the uppermost sag sequence of the South Atlantic passive margin. Field observations allows definition of four transgressive-regressive cycles characterised by fluvial to tidal-influenced mixed clastic-carbonate and carbonate-dominated deposits, that locally show evidence of evaporite dissolution; highlighting that evaporite deposition started earlier than deposition of the regional South Atlantic Loeme-Bambata evaporite formations. Two separate pre-salt carbonate units have been differentiated within the Cangulo Fm; i) a lower transitional to marginal marine, and ii) a younger upper non-marine freshwater travertine system, that is documented for the first time in the west African margin. Transgressive-regressive cycles control the early diagenesis of the tidal carbonates that include dolomitization due to mixing fluids during transgressions, and karstification due to evaporite dissolution by meteoric water circulation during regressive events. Clastic supply appears to have been completely shut down during carbonate deposition, suggesting major climatic change associated with carbonate deposition. During the lowstand between the two carbonate units, fluid flow through Cangulo palaeovalley was re-established resulting in extensive karstification and formation of a large-scale erosional unconformity that is interpreted to be time equivalent to an intra Chela-Cuvo Fm. event. The top of the studied succession corresponds to the transgressive deposits of the Bambata evaporites that are not preserved in the Cangulo palaeovalley due to its erosion but are regionally developed. The results of this study can be directly linked to along strike age equivalent Pre-Salt successions cropping out in the Namibe, Benguela and Kwanza basins, and directly offshore Angola and Brazil using well and seismic data. These new data shed important new light and constraints on the depositional and diagenetic evolution of the complex Pre-Salt reservoir systems of the South Atlantic, and the depositional and bathymetric setting at the time of onset of the main south Atlantic evaporite deposition.

1. Introduction

Sedimentary basins of the South Atlantic have been the focus of numerous publications in the last decades due to prolific hydrocarbon discoveries made from the 1950's onwards (Brownfield and Charpentier, 2006; Cameron et al., 1999; Wen et al., 2019). Pre-salt carbonates and clastics, salt-tectonic plays and post-salt carbonate and clastic systems have been explored and analysed in the Campos, Santos, Congo,

* Corresponding author. Geosciences Barcelona (GEO3BCN-CSIC), Lluís Solé i Sabarís s/n, Barcelona, 08028, Spain.
** Corresponding author. Geosciences Barcelona (GEO3BCN-CSIC), Lluís Solé i Sabarís s/n, Barcelona, 08028, Spain.
E-mail addresses: mar.moragas@uib.no (M. Moragas), jverges@geo3bcn.csic.es (J. Vergés).

https://doi.org/10.1016/j.marpetgeo.2023.106153
Received 7 October 2022; Received in revised form 28 January 2023; Accepted 30 January 2023
Available online 2 February 2023

Kwanza and Benguela basins (Fig. 1). However, the Namibe Basin of the African margin (Angola) has remained relatively underexplored compared to other west African basins and the conjugate Brazilian margin. Limited data has been published from the offshore Namibe Basin, and generally these data and descriptions have been restricted to brief inclusion in regional studies (Beglinger et al., 2012; Masse and Laurent, 2016). Since the original mapping and stratigraphic study of de Carvalho (1961), few publications have addressed the onshore geology of the Namibe Basin, such as the tectono-sedimentary evolution or volcanic activity (Jerram et al., 2019; Sharp et al., 2016; Strganac et al., 2014; Swart et al., 2016), deposition and diagenesis of Aptian evaporites and very latest pre-salt units (Gindre-Chanu et al., 2015, 2016), or the diagenetic overprint on pre- and post-salt carbonates (Fiordalisi et al., 2021; Rochelle-Bates et al., 2020; Schröder et al., 2016; Teboul et al., 2019).

Pre-Salt sag deposits in particular have received little attention to date, especially in onshore areas, where they usually appear as thin condensed successions developed on the edge of the South Atlantic rifted margin inboard of the so called Atlantic hinge zone (Fig. 2c). In this study from the onshore Namibe Basin (SW Angola), we build on the regional tectono-stratigraphic and framework mapping studies of earlier workers (de Carvalho, 1961; Sharp et al., 2016; Swart et al., 2016), and present new data and interpretations focused on the mixed clastic and carbonate sedimentary succession cropping out in Cangulo palaeovalley where initial mapping and logging had identified a well-exposed Aptian palaeovalley fill succession that offered the opportunity to study in the detail the depositional and diagenetic characteristics, sequence evolution and climatic shifts of the uppermost sag sequence from the South Atlantic margin. Documentation of these deposits can bring important new data, constraints and insights on the geological evolution of this portion of the South Atlantic passive margin, and in-turn these new data can then be placed within a broader regional South Atlantic understanding.

This study aims to characterise the Early Cretaceous (Aptian) mixed clastic and carbonate sedimentary succession in Cangulo palaeovalley to better understand the sedimentary and diagenetic evolution of the uppermost sag sequence from the South Atlantic margin. Specifically, the objectives of this study are: (i) to characterise the lithostratigraphy and depositional facies of the succession with special emphasis on the Cangulo Fm. carbonates, (ii) to characterise the petrology of host rocks, and (iii) to characterise the geochemistry (elemental and carbon-oxygen isotopes) of host rocks and diagenetic products. Observations from this limited area onshore have important implications for understanding offshore pre-salt reservoirs.

2. Geological setting

2.1. The Cretaceous evolution of the Namibe passive margin

The Namibe Basin is the southernmost of the Angolan basins, bordered by the Walvis-Rio Grande Ridge to the south and the Benguela-Kwanza Basin to the north (Fig. 1). This part of the continental margin of Angola developed during Early Cretaceous breakup of Pangea, which led to the formation of the Atlantic Ocean (Reston, 2010; Schettino and Scotese, 2005). The separation of the two conjugate South Atlantic margins, Africa, and South America, was characterised by the development of thick rift successions during the Early Cretaceous, with asymmetrical horst-and-graben structures developed parallel to the present coastline and affecting both Precambrian basement and early rift igneous deposits of the Paraná-Etendeka volcanic complex (Guiraud et al., 2010). Data from the Kwanza Basin indicates rift topography was filled by continental-lacustrine deposits, accompanied by a locally

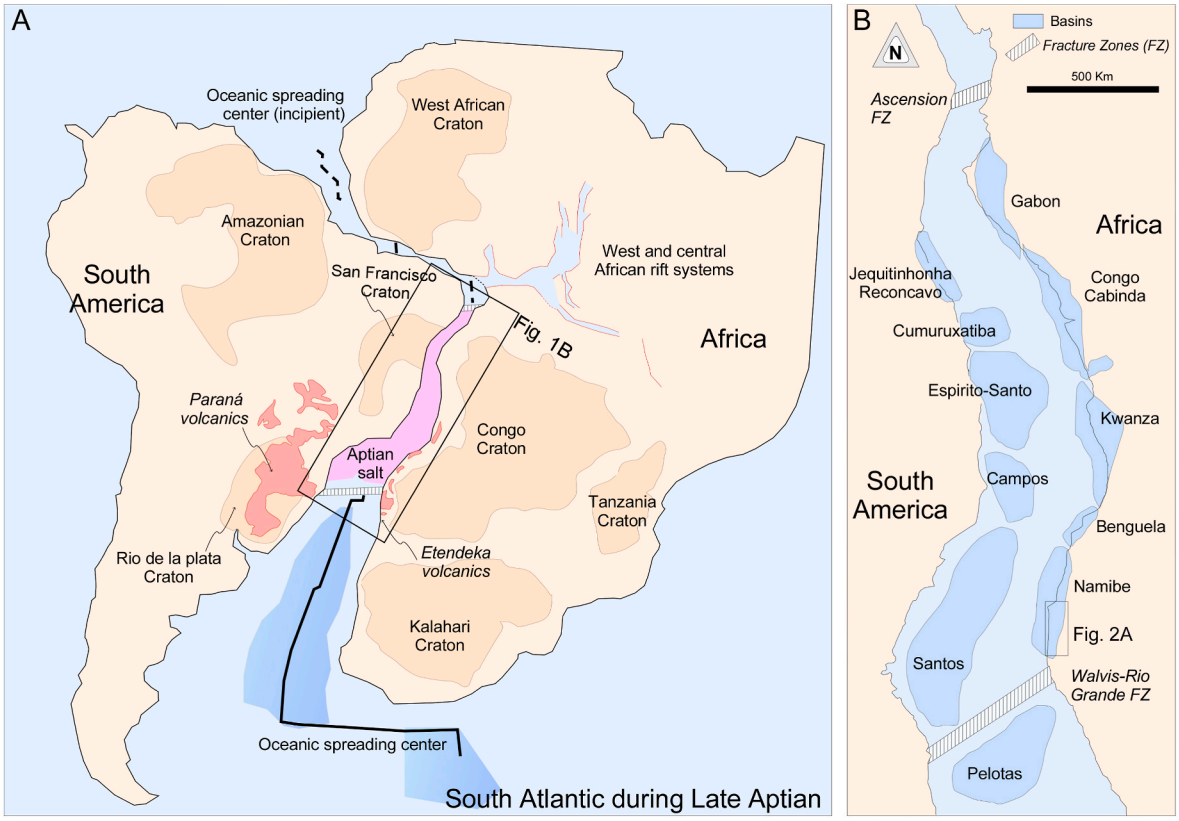

Fig. 1. A) Paleogeographic map at Late Aptian times in the South Atlantic region showing distribution of the early rift volcanic Paraná-Etendeka provinces (Hauterivian-Barremian) and Aptian salt deposits (based on Globig et al., 2016; Heine et al., 2013; Moulin et al., 2013; Pérez-Díaz and Eagles, 2014). B) Distribution of South Atlantic basins including location of the paleogeographic position of the Namibe Basin.

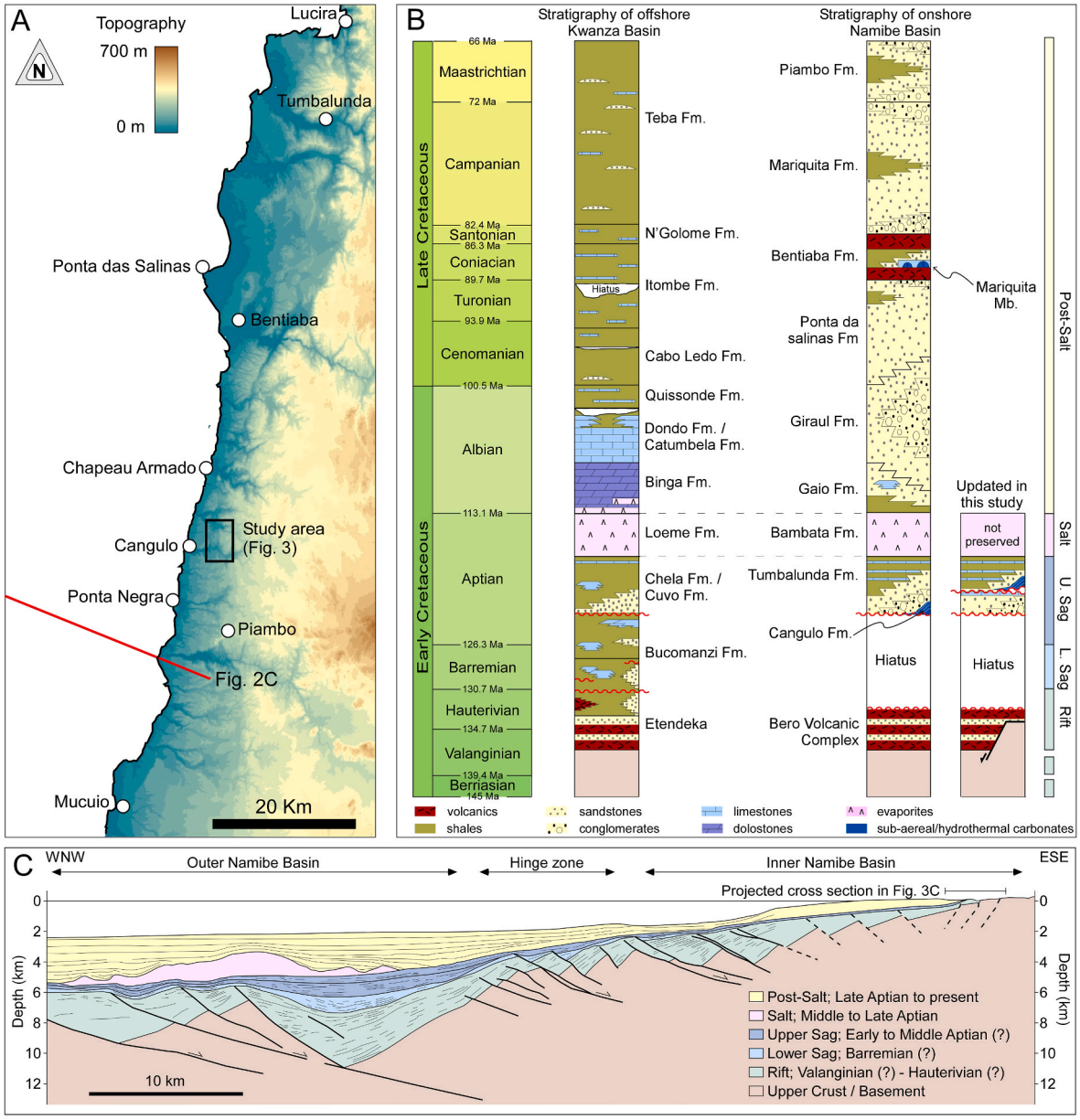

Fig. 2. A) Topographic map of Namibe Basin (SW Angola) showing the location of Cangulo valley. Comparable palaeovalley successions to Cangulo have been mapped in the Piambo, Ponte Negra, Chapeau Armado, Bentiaba, Tumbalunda and Bero regions of the Namibe Basin. B) Chronostratigraphic chart of the onshore Namibe Basin and interpreted offshore equivalent units based on offshore Kwanza Basin data (Brownfield and Charpentier, 2006; Burwood, 1999; Gindre-Chanu et al., 2015; Guiraud et al., 2010; Jerram et al., 2019; Sharp et al., 2016; Swart et al., 2016). C) Interpreted partial seismic line modified from Higgins et al. (2016) and Sharp et al. (2016) showing the main seismic sequences defined in the offshore Namibe Basin. Preliminary age assignment is made by correlation to Benguela and Kwanza basin wells to the north. The onshore sections described in this paper occur at the easternmost part of this section. Significant volcanic addition, SDR's and oceanic crust are evident immediately to west of section (not shown) based on seismic facies and gravity/magnetic data, indicating the Namibe rifted margin is very narrow. Note low angle landwards dipping faults that are sealed by latest sag units. 2DPSDM GXT CongoSPAN line 800 seismic data proprietary to TGS.

significant volcanic component. In Namibe, the Paraná-Etendeka age equivalent Bero Volcanic Complex is dated between 130 and 134.5 Ma in onshore sections (Marsh and Swart, 2018; Torsvik et al., 2009), and is exposed as a series of flat lying units sitting direct on basement, or more typically as a well exposed series of rotated fault blocks and half grabens, with evidence for syn-depositional fault movement and local ponding of igneous units (Sharp et al., 2012, 2016). Age equivalent highly faulted igneous successions are also evidenced at outcrop in the onshore Kwanza Basin (Jerram et al., 2019; Marzoli et al., 1999). Thick clastic-dominated lower and lowermost upper sag successions are absent onshore Namibe and Kwanza but are well imaged on seismic data and proven in well bores in the immediate offshore outboard of the main Atlantic hinge zone (Fig. 2). Regionally, the sag phase was characterised by significant crustal thinning and subsidence, but with limited extensional faulting occurring in the inboard areas whilst the outboard areas continued to undergo active extension and rifting, through to at least Loeme Fm evaporite deposition times in the offshore Namibe and Outer Santos basins (Karner et al., 2003 Quirk and Rüpke, 2018; Higgins et al., 2016).

In the onshore Namibe Basin, the Precambrian basement and Bero volcanics are unconformably overlain by an onlapping and overstepping mixed carbonate-clastic succession assigned to the uppermost Upper sag (Fig. 2). These sediments, which are the latest Pre-Salt deposits, are lithostratigraphically termed the Grey Cuvo in Angola, and Chela or

Gamba Fm's further north in West Africa (Brownfield and Charpentier, 2006; Burwood, 1999; Marton et al., 2000; Van Eden, 1978). In the onshore Namibe Basin these units have been termed the Cangulo and Tumbalunda formations (Gindre-Chanu et al. 2016). The Upper sag onshore succession dips and expands progressively offshore, locally steepening across lineaments (Fig. 2). The onshore Upper sag sedimentary package is relatively thin and encountered in well-developed incised palaeovalleys, suggesting a significant period of exposure between deposition of the Early Rift volcanics and latest sag units (Gindre-Chanu et al., 2016). The palaeovalley fill successions are up to 150 m thick, but thin markedly to between 5 and 20 m thick on intervening interfluves. The latest Pre-Salt sag deposits onshore Namibe Basin comprise a complex suite of interbedded subaerial to subaqueous carbonates (Cangulo Fm.) and continental and transitional clastics (Tumbalunda Fm.) that are poorly aged-constrained, but regionally are overlain by the Aptian-aged evaporites of the Loeme-Bambata formations (Rochelle-Bates et al., 2020; Sharp et al., 2016). The uppermost Tumbalunda Formation is composed of a set of siliciclastics, evaporites and carbonate beds informally named the "Lower evaporite unit" (Gindre-Chanu et al., 2016). In this unit, thinly laminated stromatolites, gypsum, and mudstone beds are interbedded with metre to decametre-thick coarsening-upward units made up of sandy marlstone and cross-bedded pebbly to cobbly sandstones interpreted as marine shallowing-upward deltaic and intertidal to sabkha packages (Gindre-Chanu et al., 2016). A regionally occurring 5 m thick highly altered evaporite with evidence of evaporite dissolution typically marks the base of this "Lower evaporite unit". The overlying Loeme-Bambata evaporites are an up to 70 m thick package of gypsum and anhydrite, with evidence of significant karstification and evaporite dissolution (Gindre-Chanu et al., 2015). In localities where evaporites are preserved, they pass upwards to the Albian post-salt marine clastic and restricted evaporitic carbonates of the Gaio Fm., age and facies equivalent to the well-known Binga Mbr within the Pinda Group of the Kwanza Basin (Schröder et al., 2016). This Early Albian marine transgressive event above the main evaporites is a well-known super regional event in the South Atlantic Basins. Gaio Fm. Marine deposits are abruptly and often erosionally overlain by a thick Albian to Early Cenomanian succession of fluvial to alluvial clastics of the Giraul Fm. that pass progressively basinwards into marine carbonates (Fig. 2). These units are time equivalent to marginal to non-marine clastics of the Dondo Fm that pass basinwards into marine deposits of the Catumbela Fm in the Benguela and Kwanza basins (Quesne et al., 2009). The Giraul Fm records a significant regressive event in the Namibe Basin associated with clear large scale basinwards rotation. Significant intra Albian evaporite dissolution and karstification of Gaio Fm. Carbonates can be demonstrated in association with this regressive and rotational event in Namibe (Gindre-Chanu et al., 2016; Sharp et al., 2016). A Late Cenomanian to Turonian transgression resulted in the deposition of the Ponta da Salinas Fm. over the Giraul Fm. continental deposits that terminated with the emplacement of Coniacian Bentiaba Basanite Fm. (around 88 Ma according to Jerram et al., 2019), and coeval deposition of locally developed subaerial carbonates (Mariquita Mb. In Fiordalisi et al., 2021). Volcanics and sediments of the Bentiaba Fm. are onlapped and overstepped by a Santonian to Campanian clastic succession (Mariquita Fm. In Fig. 2) that is composed of a transgressive-regressive sequence of shelf margin, shoreface to deltaic sediments. The Cretaceous terminates with a Maastrichtian transgressive-regressive cycle in the Namibe Basin recorded by clastic deposits of the Piambo Fm. (Sharp et al., 2016; Swart et al., 2016). Eocene, Miocene and Pliocene shelfal to shoreface successions form the youngest outcropping units in onshore southern Namibe (de Carvalho, 1961).

2.2. Cangulo palaeovalley

Renewed mapping work across the entire Namibe Basin onshore margin was undertaken during 2010–2013 and has been tied to the offshore via 2D and 3D seismic lines (Equinor, 2011; Sharp et al., 2016; Swart et al., 2016). From this regional onshore work, special focus was placed on areas where the sedimentary record was most complete, that typically occurs in the vicinity of long-lived palaeovalley. The Cangulo river valley offers one of the best exposures of a Pre-Salt paleovalley fill and was the subject of this detailed study.

The Cangulo palaeovalley, located in the central part of Namibe Basin (Fig. 2), is interpreted as a Cretaceous-aged palaeovalley incised into crystalline basement that has a composite fill of both pre- and post-salt sediments. Regional onshore mapping in the Namibe, Benguela and Kwanza basin (Equinor, 2011; Sharp et al., 2016; Swart et al., 2016) has revealed a series of comparable palaeovalleys developed all along the Angolan rifted margin. The valleys are typically observed eroded into both Precambrian basement and into an irregular erosional landscape developed at the top of the Bero/Etendeka 131-134 Ma volcanics. The palaeovalleys are typically filled by Aptian-Albian aged sediments, locally including Loeme-Bambata Fm. evaporites. The onshore palaeovalleys can be mapped into the offshore on 2D and 3D seismic datasets, where they are filled by pre-salt Sag successions with fills in the order of 150–300 m (Higgins et al., 2016; Sharp et al., 2016). In both onshore and offshore sections, the same palaeovalley features can be observed to have been repeatedly reutilized, filled by post-salt Albian, Santonian, Campanian, Maastrichtian, Cenozoic, and modern drainage systems. These observations indicate West African drainage is largely antecedent in nature, with the palaeovalleys reused multiple times through the geological record (Sharp et al., 2016; Higgins et al., 2016).

The above age relationships indicate a predominant phase of palaeovalley cutting that occurred post Etendeka (131-134 Ma) followed by composite filling that occurred predominantly during the Aptian, Albian and younger. Outcrops in the southern onshore Namibe Basin (Bero River area) however, indicate a probable even older origin for some of the Namibe Basin palaeovalley network, with a well exposed valley fill clastic succession of fluvio-lacustrine-glacial affinities (including varved facies with striated dropstone like clasts) sealed by overlying relatively flat lying Etendeka volcanics (131-134 Ma, Equinor, 2011). This situation is comparable to Carboniferous-Permian glacial valley fills described along the Angolan-Namibian border (Cunene River), NW Namibia and in South Africa, where Carboniferous-Permian glacial sediments of the Dwyka Fm. fill deep glacial valleys and are overlain by Etendeka volcanics (Isbell et al., 2008; Swart et al., 2016; Dietrich et al., 2021). These valley systems, like those exposed in Angola, are reutilized by successively younger drainage systems up to and including the present-day drainage network.

In the case of Cangulo palaeovalley, the valley base and sides comprise fractured and faulted basement of Precambrian granitic and metasedimentary rocks that constitute the Angolan Shield – southern Congo Craton (De Carvalho et al., 2000; McCourt et al., 2013; Szatmari and Milani, 2016). The basal sedimentary infill of the Cangulo palaeovalley comprises Aptian-aged Pre-Salt Tumbalunda and Cangulo Formations (Fig. 3). The overlying post-salt sediments of the Gaio-Giraul (Pinda Group equivalent), Ponta da Salinas, Bentiaba, and Piambo Formations directly overlie the Pre-Salt deposits, without any remnants of the Bambata Fm. evaporites between them (Fig. 3). Although not preserved in the studied valley, deposition of Bambata evaporites is recorded regionally. Equivalent exposures in the Chapeau Armado and Ponte Negra palaeovalleys, and in the Tumbalunda, Gaio and Piambo localities (Fig. 2) still preserve remnants of the original salt layers (Gindre-Chanu et al., 2015, 2016). Within the Chapeau Armado palaeovalley spectacular 100–150 m thick salt-tectonic and syn-halokinetic growth strata are exposed in the Albian section, testifying to an originally thicker evaporitic (halite?) valley fill. In general, remnant gypsum-anhydrite is typically thicker (40–50 m) and better preserved along strike outside of the individual palaeovalleys (i.e interfluve locations). This may reflect greater freshwater flow and dissolution of the evaporites within the palaeovalleys, such as the Cangulo Palaeovalley, compared to the interfluves (Gindre-Chanu et al., 2016; Sharp et al.,

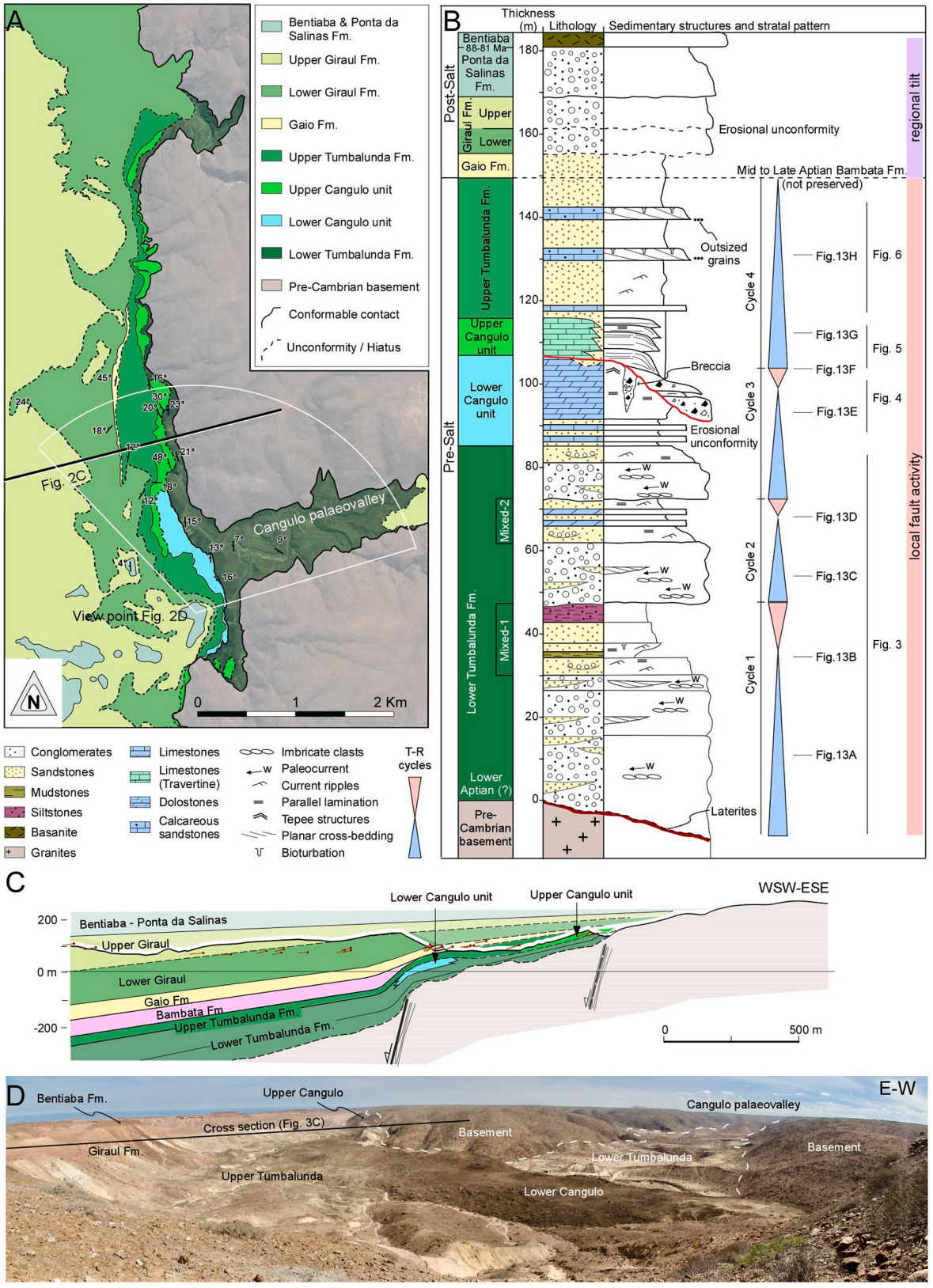

Fig. 3. A) Geological map of Cangulo palaeovalley based on fieldwork integrated with remote sensing mapping; B) General stratigraphic log for the studied area showing the Cangulo palaeovalley infill and the interpreted transgressive-regressive parasequence sets; C) Cross-section of the eastern termination of Cangulo Valley. Evaporites of Bambata Fm. are not present in Cangulo palaeovalley but are interpreted to be present at depth in the cross section (see section 2.2 for details). D) Panorama looking updip into Cangulo palaeovalley showing the distribution of the outcropping sedimentary units. Based on tectono-stratigraphic and tectono-topographic relationships, we interpret west-dipping normal fault zones as active during early deposition in the region followed by large-scale tilting of the entire Early Cretaceous post-salt succession observed by its regional wedge geometry. Approximate position of the viewpoint and area shown in A).

2016).

From the Pre-Salt deposits in Cangulo palaeovalley, focus of this study, the older unit correspond to the Tumbalunda Fm. (Fig. 3). Regionally within the onshore Namibe Basin, the Tumbalunda Fm comprises continental, lacustrine to transitional clastic marine deposits that display an overall transgressive fining upward trend that progressively onlaps and oversteps the Precambrian basement, ending with deposition of Aptian evaporites of the Bambata Formation (Gindre-Chanu et al., 2016). The overall transgressive trend of the Tumbalunda Fm. is punctuated by individual flooding surface bound progradational-regressive cycles (parasequences), that collectively stack into a number of well-defined progressively deepening-backstepping cycles (i.e a transgressive parasequence set). Individual parasequences are fluvial dominated in the upper reaches of the palaeovalleys, and display more marine to tidal indicators in their lower reaches. This large-scale transgressive, backfilling, fining upwards trend, and up-dip fluvial to down-dip marine facies change, is also evident in palaeovalleys studied in the Benguela and Southern Kwanza basins, and is particularly well exposed in the Benguela Basin (Sharp et al., 2016). In the Cangulo palaeovalley, several high order transgressive-regressive parasequences are identified within the Tumbalunda Fm. (Fig. 3). In contrast to other sections however, the Tumbalunda Fm. has here been subdivided in two distinct intervals (Lower and Upper) separated by carbonates of the Cangulo Fm. (Fig. 3).

The Cangulo Fm., originally interpreted to be time equivalent to the lowermost Tumbalunda Fm. (Fig. 2B), was previously described as comprising non-marine fissure- and fault-fed spring carbonate systems laterally passing to lacustrine and marginal marine mixed carbonate-clastic successions. This formation passively drapes top basement and top Bero volcanic units, and interfingers with clastics of the Tumbalunda formation (Rochelle-Bates et al., 2020). In the Cangulo palaeovalley, we differentiate two distinct carbonate intervals within the Cangulo Fm., named Lower and Upper Cangulo units in Fig. 3, separated by a major newly recognised unconformity. The Upper Cangulo unit, identified in a higher stratigraphic position than previously reported (Fig. 2B), interfingers with and is overstepped by clastics and carbonates of the Upper Tumbalunda Fm., which has an overall transgressive nature up to the contact to the Bambata Fm. evaporites, not preserved in the Cangulo palaeovalley (Fig. 3).

3. Methodology and database

The geology of Cangulo palaeovalley was characterised through a combination of remote sensing mapping (RSM), fieldwork and laboratory analysis. Remote sensing mapping was performed using Equinor-Digitizer2, software, using very high resolution orthorectified satellite imagery, and a digital elevation model (DEM) with a resolution of 1.0 m. RSM and field mapping were supported by the interpretation of stratal relationships directly onto field photopanoramas.

Fieldwork was undertaken to collect systematic structural (strike and dip), stratigraphic, lithologic and sedimentological (facies) data. The stratigraphic work includes 200 m of logged sections in both pre-and post-salt successions, accompanied by three detailed logged sections within the Pre-Salt carbonate units (Fig. 3). Field work included the collection of more than 160 samples for depositional, petrology and diagenetic analysis of carbonate intervals, with an additional 20 samples for clastic intervals.

Some 119 standard and polished thin sections were studied from selected samples to constrain depositional and diagenetic phases. Petrographic observations were made using optical and cathodoluminescence microscopy. A CL TECHNOSYN Cathodoluminescence device Model 8200 MkII operating at 23 kV and 350 μA gun current was used to distinguish depositional and diagenetic phase generations. Porosity quantification was made directly from thin-section using ImageJ software (Rasband, 1997) to calibrate against observations made directly in the field.

Carbon-coated polished thin sections were used to analyse major, minor and trace element concentrations on a JEOL JXA-8230 electron microprobe. The equipment was operated using 20 kV of excitation potential, current intensity of 6 nA for Ca and Mg, and 40 nA for Mn, Fe and Sr, with a beam diameter of 10 μm. Detection limits are 236 ppm for Ca, 397 ppm for Mg, 226 ppm for Mn, and 78 ppm for Fe. Precision on major element analyses averaged a standard error of 6.15% at 2σ confidence levels.

52 microsamples of carbonate phases, identified on thin section and collected by microdrilling, were prepared to determine the carbon and oxygen stable isotope ratio. Calcite and dolomite powders were reacted with 103% phosphoric acid for 10 min at 90 °C. The CO_2 was analysed using an automated Kiel Carbonate Device attached to a Thermal Ionization Mass Spectrometer Thermo Electron (Finnigan) MAT-252. The isotopic results have a precision of ±0.02‰ for $\delta^{13}C$ and ±0.04‰ for $\delta^{18}O$. The results were corrected using the standard technique (Claypool et al., 1980; Moore and Wade, 2013) and are expressed in ‰ with respect to the VPDB standard.

Mineralogical composition of 12 samples was determined by X-ray diffraction (XRD) measurements performed with a Bruker D8-A25 diffractometer equipped with a Cu tube (lambda = 1.5405 Å) and an ultrafast position sensitive detector (PSD). XRD scans were collected over the 2θ range between 4° and 70° with steps of 0.035° and an equivalent integration time of 96 s per step. A voltage (current) of 40 kV (40 mA) was applied to the x-ray generator. The phases in the samples were identified with Bruker's software package Diffrac.Suite™ together with the PDF-2 database from the International Centre for Diffraction Data (ICDD).

4. Results

4.1. Stratigraphy and lithofacies

4.1.1. Basement and pre-Lower Tumbalunda Fm

The basement of the study area, Precambrian in age, is made of granitic and metasedimentary rocks. These rocks are commonly weathered in outcrop exposures, locally forming well-developed laterites rich in botryoidal goethite up to 5 cm-thick and scree deposits (Fig. 4A and B). Pre-Tumbalunda scree deposits consist of particulate rubble floatbreccia formed by angular mm to cm-reworked fragments of the crystalline basement. The matrix of the breccia contains reworked micro fragments of the basement, clay minerals and iron oxides that locally gives a lateritic aspect to these sediments.

4.1.2. Lower Tumbalunda Fm

The Lower Tumbalunda Fm. progressively onlaps and overlies the Precambrian basement towards the east and is organized in three finning and thinning upwards cycles (Fig. 3).

Unconformably above the basement, the first cycle (Fig. 3) initiates with moderately sorted and clast supported red conglomerates made of rounded clasts, which can reach up to 2 m in diameter, with a dominant granitic lithology and minor quartzite and metavolcanics. Above, the conglomerates pass upwards to a sand-dominated interval made of channelized and sheet-like coarse grained sandstones with conglomeratic interbeds (Fig. 4C). The sandstones show abundant current ripples, rarely wave ripples, and primary current lineation (PCL). Measured paleocurrent and clast imbrication in the basal conglomerate indicate a predominance flow to the west. This first cycle is capped by a 20 m thick sandstone to siltstone-dominated interval that includes a distinct and locally mappable green mudstone (Mixed-1, Fig. 4C). The sandstone and siltstone beds are characterised by bi-directional current and climbing ripples, flaser to lenticular bedding, tool marks, load structures, PCL and both grazing and dwelling (?bivalve resting) ichnofabrics. Low angle channel scours are also evident, with the channels filled by bi-directional cross bedded and current rippled sands and silts, locally homogenized and thoroughly bioturbated.

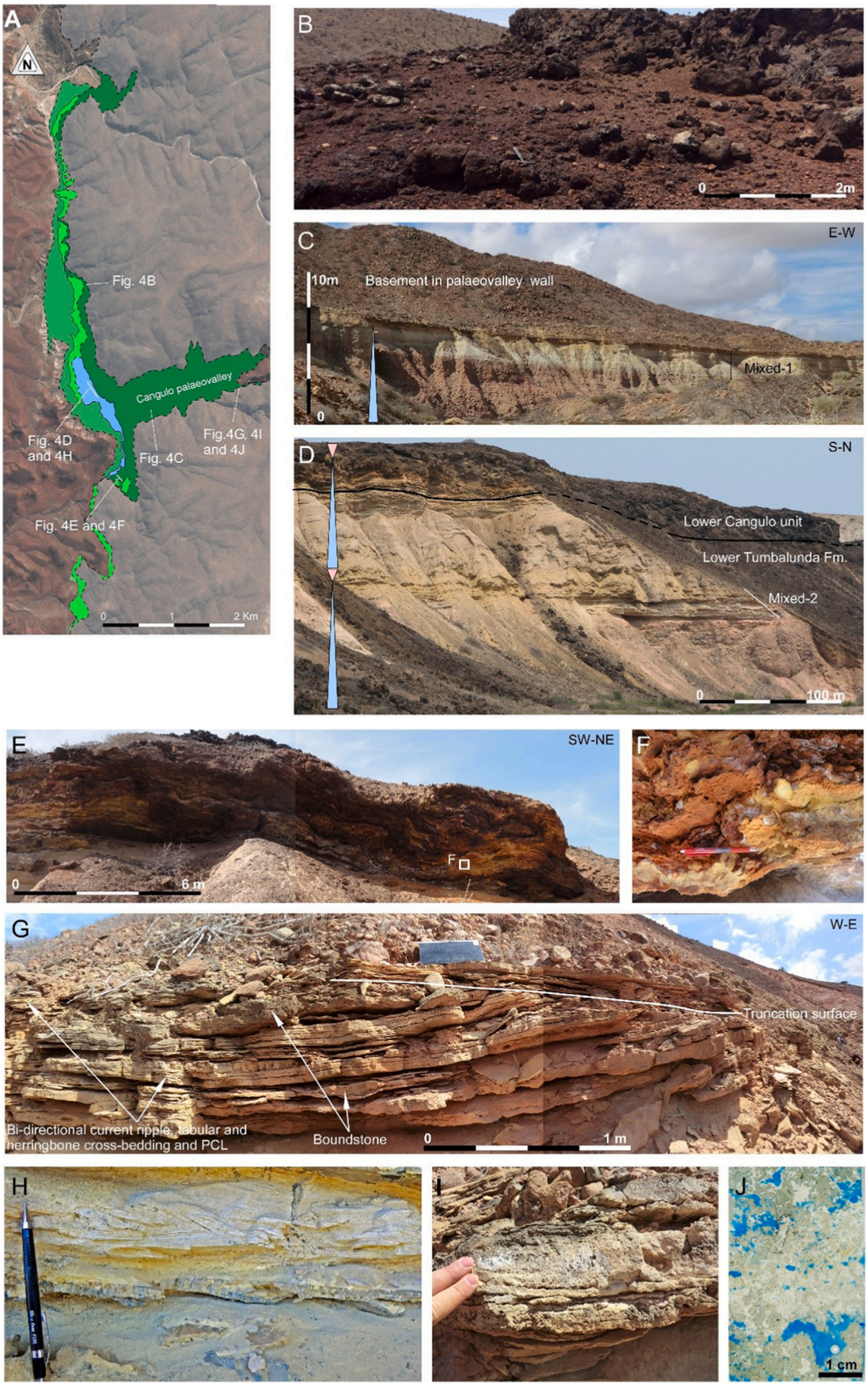

(caption on next page)

Fig. 4. A) Simplified geological map of Cangulo palaeovalley showing the distribution of Pre-Salt formations and the location of pictures shown in this figure. B) Outcrop photograph showing the well-developed laterites developed over Precambrian basement. C) Photograph showing the lowermost part of the Lower Tumbalunda Fm. outcropping in Cangulo palaeovalley corresponding to the first identified cycle. Note the abrupt change between red conglomerate and yellowish fine-grain dominated intervals. D) Outcrop photograph showing the main characteristics of the second cycle of Lower Tumbalunda Fm. composed of basal red conglomerate transitioning upwards to the carbonate-clastic interval (Mixed-2). E and F) Outcrop and detailed photograph of the highly altered iron-Mg-sulphur rich interval laterally equivalent to the Mixed-2 interval. G) Outcrop photograph showing the main sedimentary features of the clastic portion of the Mixed-2 interval characterised by truncation surfaces, herringbone cross bedding, planar cross lamination and bi-directional ripples (H). These clastics are accompanied by microbial boundstones. I and J) Detail outcrop photograph and thin-section scanned of microbial boundstones encountered in the Mixed-2 interval.

The second depositional cycle (Fig. 3) begins with moderately sorted red to yellow conglomerates (Fig. 4D), characterised by a channelized and strongly erosive base. It is internally organized into several multi-story and laterally stacked conglomerate filled channels. The conglomerate shows a consistent westward paleocurrent based on clast imbrication. Upwards, conglomeratic deposits gradually change to texturally immature sandstones with abundant current and wave ripples, PCL and shallow conglomerate filled scours and sheets. The sandstones are poorly sorted, show abundant clay matrix (illite and kaolinite), and present angular to sub-angular quartz, feldspar (predominantly microcline) and chlorite grains (see X-ray diffraction results in supplementary material, Table 1). They are texturally and compositionally immature. The top of the cycle is made of a 5 m thick distinctive mixed carbonate-siliciclastic interval (Mixed-2 in Fig. 4D) that forms a laterally continuous and traceable horizon eastward up into the interior of the Cangulo palaeovalley. In the southern and northern part of the Cangulo outcrop belt, a highly altered Ca and Fe-sulphur rich interval (Gypsum and Jarosite >30%, according to X-ray diffraction) is interbedded with the carbonates and clastics of this interval (Fig. 4E and F). The sandstones include abundant climbing and bi-directional ripples, mud drapes, and very well-developed herringbone and ripple cross bedding. Within the sandstones, channelling, internal scours and truncation/reactivation surfaces are common (Fig. 4G and H), with mud-chip clasts lining the scours. Laterally, migrating cross bedded mixed carbonate-clastic facies fill individual channels. Grazing and resting traces are evident on sandstone bases. Planar to PCL bedded intervals are also developed between the cross bedded and channelized facies. The interbedded carbonate beds (Fig. 4I and J) comprises cm to dm thick dolomitized and partially silicified algal boundstones characterised by laminar, domal to radial morphologies and locally tepee structures. The boundstones are developed along the tops of cross bedded sands. The mixed carbonate-clastic-evaporitic section is overlain by a poorly exposed light grey sandstone with distinct load, ball and pillow and flame structures.

The third depositional cycle (Fig. 3) has a similar sharp, erosive conglomerate filled basal contact as cycle 2, and is overlain by an overall fining upwards sandstone succession as well. To the south and east (up the palaeovalley) red conglomeratic channelized facies dominate, whilst in the main cliff section to the west channelized conglomeratic sandstones with large scale cross bedding, dewatering and load structures are evident. This unit has a gradational upward contact to thinly interbedded succession of sandstones, siltstones and mudstones with well-developed planar, current, flaser, lenticular, and tabular trough cross bedding. Distinctive mud drapes, and intervals with intraformational rip-up clasts are common, as is evidence for flow reversal. Shallow (10–50 cm deep) cut and fill channels with heterolithic rippled infills and rip-up clasts at channel bases cut the succession. The contact with the overlying Lower Cangulo unit is gradational, marked by the progressive appearance of interbedded dolomitic carbonates with well-developed laminar, crinkly, fenestral to locally domal and algal morphologies interbedded with siltstones, mudstones and thin fine-grained sandstones, forming very rhythmic cm scale cycles. Tepee and mud-chip rip up horizons are locally developed. Bedding parallel gypsum veining is also quite common.

4.1.3. Lower Cangulo unit

The Lower Cangulo unit crops out at the western termination of Cangulo palaeovalley, lying conformably above the Lower Tumbalunda Fm (Fig. 3). This succession comprises 15 to 20 m-thick dolomitised carbonate deposits. These are laterally continuous towards the mouth of the palaeovalley (Fig. 5A). Given the coarse and immature nature of the underlying Lower Tumbalunda siliciclastics contained within the Cangulo palaeovalley, as described above (Figs. 3 and 4), it is remarkable that the Lower Cangulo carbonates are deposited within and extend up the main palaeovalley axis.

The top of the Lower Cangulo unit is locally karstified with localised collapse breccias, caves, breccia pipes and evidence of large-scale lateral accretion (Fig. 5B). In order to characterise depositional and karstic characteristics of the Lower Cangulo unit, two stratigraphic sections were logged and sampled (SCS1 and SCS2, Fig. 5C and D respectively), and walked out laterally into karstic breccias, cavern fills and even large-scale lateral accretion surfaces towards the mouth of the palaeovalley. The two sections are described below.

The SCS1 section exemplifies the original depositional facies and stratigraphic architecture of the Lower Cangulo carbonates (Fig. 5C). The SCS1 section is placed in a gentle antiformal high and here the impact of the paleokarst is minimal, and bedding is subhorizontal. Laterally, the Lower Cangulo unit thins away from the SCS1. The SCS1 section is 15 m-thick and is made of cm-to dm-thick dolostone beds with irregular base and top, occasionally showing a low relief dome shape (Fig. 5E), cross lamination and tepee structures (i.e., microbial?), interbedded with few cm-thick yellow sandstones. Dolostones appear as two main unfossiliferous microfacies, laminated and non-laminated, both yielding less than 15% of porosity with dominant types being fenestral and centimetre-scale vug porosity. The fenestral porosity appears to be primary, while vuggy porosity appears to be secondary, related to karst processes. It is also unclear if the thin intercalated sandstone is primary or a secondary fill following karstification as within section sands are also observed to fill vugs and small karst pockets. Along strike, m-scale sandstone are intercalated within paleocaverns formed in the formation.

The section is dominated by laminated mud-wackestones that are thoroughly dolomitised. The laminated microfacies is characterised by up to 1 cm-thick planar to wavy laminae of dolomitised mudstones and mm-thick ochre-coloured laminae made of fine-grained quartz and iron oxides (Fig. 5F). Fenestral porosity is aligned following the lamination towards the top of the section where tepee-like structures are also present. The non-laminated microfacies correspond to dolomitised limestone containing heterogeneously distributed mm-size and undifferentiated sub-rounded non-skeletal components, commonly dense packed, exhibiting a clotted appearance (Fig. 5G). Locally, this microfacies include intervals with ghosts of polygonal-shaped components interpreted as pseudomorphs of evaporite crystals (Fig. 5H). Other minor components such as opal, iron oxide as well as detrital quartz have been observed.

In contrast to SCS1, the SCS2 section represents a highly karstified succession of the Lower Cangulo unit. The base of the section is characterised by 1 to 4 m-thick thinning upwards cycles dominantly made of breccias (Fig. 5D and I). The base of the cycles is formed by a reverse-graded rubble float breccia composed of monomictic (host rock dolostones) and heterometric angular clasts ranging in size from 5 to >80 cm, and a karstic fill sediment comprising yellow to red silty matrix rich in iron oxides. The rubble float breccias change to mosaic and to crackle pack breccia upwards within the cycle (Fig. 5I), representing a decrease in the degree of brecciation, which is associated with a decrease in the

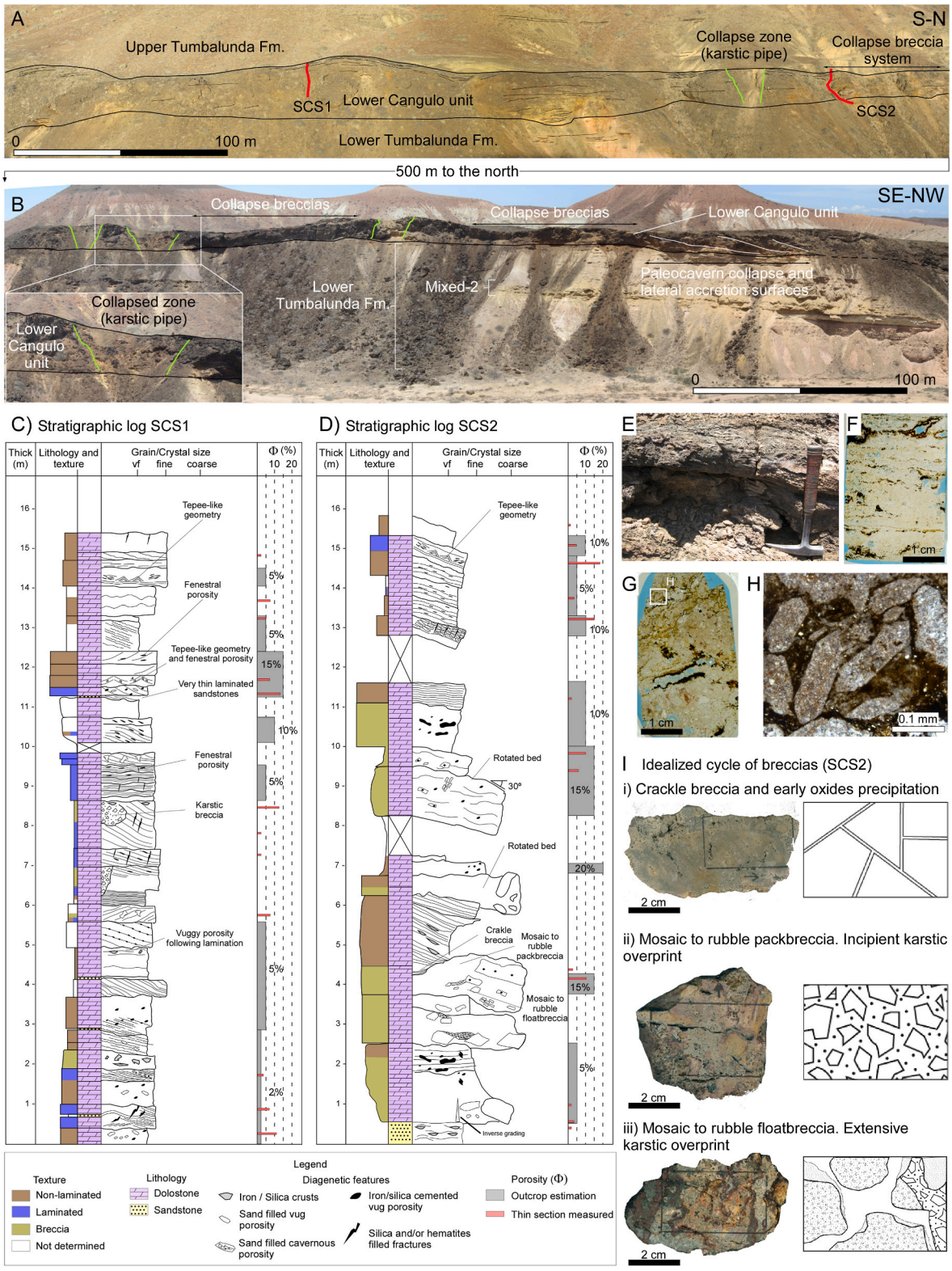

Fig. 5. A and B) Outcrop panoramas showing the lateral continuity of Lower Cangulo unit, with an increasing karstic overprinting towards the north. A) Section located to the south of the Cangulo palaeovalley where there are subtle lateral thickness changes. In these areas the carbonates contain highly rotated strata and paleocaverns as recorded in SCS2. The lateral thickness changes are as such interpreted to reflects burial collapse of the karst system developed within the lower Cangulo carbonate unit. B) section cut by several breccia pipes interpreted to be collapsed paleocaverns. They have crackle and mosaic breccia on their margins. To the north the section comprises intercalated breccias and sandstones that form low angle accretion surfaces. These strata are interpreted to represent the fluvial fill of a collapsed paleocavern,. C and D) Stratigraphic logs of non-karstified (SCS1) and karstified (SCS2) Lower Cangulo. E to H) Outcrop, thin section and microscope images showing the depositional characteristics of Lower Cangulo facies. I) Sample images and sketches showing the variability of karstic overprinting observed in Lower Cangulo unit.

content of silty matrix and space between angular clasts. The upper 9 m of the section are beds rotated to c. 30° through collapse of the paleocavern roof.

Petrographic observations show that the composition of clasts within the different types of breccias and of the uppermost beds of the cycles are equivalent to the depositional microfacies of the SC1 section. Field estimations and thin section quantification indicate a heterogeneous distribution of porosity values varying from 2 to 15%. As in the SCS1 section, two main porosity types have been differentiated in the more karstified Lower Cangulo succession, vuggy and fenestral porosity. Vuggy porosity is the predominant type observed in the basal and middle part of the unit, becoming large-size pores (cavernous porosity) in the lowermost part of the karstic cycles where dissolution is more intense. The vuggy pores have a partial fill of yellow and ochre sandstones, interpreted to be linked to subaerial exposure. Fenestral porosity is less abundant than in the SCS1 section but, when observed, mostly appears in the beds where original depositional facies are preserved.

4.1.4. Upper Cangulo unit

The Upper Cangulo unit is represented by a series of unconnected lobate carbonate bodies arranged attached to the basement north and south of the main Cangulo palaeovalley (Figs. 3, 6A and 6B). As can be observed in map pattern (Fig. 3), to the north and south of the Cangulo palaeovalley, these carbonates locally sit directly onto the fractured Pre-Cambrian basement rocks. However, traced into the axis of the palaeovalley they occur within the Tambulunda Fm. In proximity of the palaeovalley, the base of the Upper Cangulo unit is marked by a major and locally high angle unconformity that is superbly exposed (Fig. 6A). These carbonates, predominantly limestones with some dolostone intervals, are characterised by an unconformable erosive base above both the Lower Tumbalunda Fm. and Lower Cangulo unit. These laterally discontinuous carbonate bodies have rapidly changing dips and locally pass laterally into clastic sediments of the Upper Tumbalunda Fm. (Fig. 6). They appear to also locally onlap against collapsed caverns and breccias of the Lower Cangulo unit (Fig. 7A).

Individual carbonate bodies reach a thickness up to 20 m and are organized in dm-to m-thick beds. Typically, the bedding is subhorizontal or dips gentle towards the west in the proximity of the basement. Westward, the dip changes rapidly to 30-40° first, and to subhorizontal later where the carbonates are interfingered with the siliciclastic deposits of the Upper Tumbalunda Fm. This abrupt change of dip is marked by a change in rock fabrics and appears to occur across a distinctive erosional escarpment but into the underlying Lower Tumbalunda Formation (Fig. 7). Locally, some of the carbonate bodies show intervals characterised by subhorizontal beds with internal cm-thick lamination (Fig. 6C), or dm-thick beds that change abruptly from flat to a steeply dipping angle (>60°, Fig. 6D).

The Central Cangulo Section (CCS, in Fig. 6E), which is considered as a reference for time equivalent geobodies in the Cangulo palaeovalley, is a 12-m-thick carbonate succession composed of dm to m-thick beds. This section is locally relatively steeply dipping and thins dramatically to the west as dips flatten out into a toe-of-slope setting. The base of the section is made of 2 m of dolostones arranged in cm to dm-thick beds characterised by laminated and non-laminated microfacies of dolomitised limestones, like facies observed in the Lower Cangulo unit, and thus interpreted to be part of this formation (Fig. 6B and E). The latter interval is karstified and shows dissolution enlarged vuggy pores that resulted in porosity values ranging between 5 and 20%. The pores are partially filled by yellow fine grain sediment (Fig. 6F).

Up section, the CCS is characterised by 10.5 m of limestone with an irregular base and flat top, showing bed-parallel to oblique lamination. The limestones appear as two main facies, massive porous and dolomicrite-microsparite crusts. The massive porous limestones facies is predominant and is characterised by massive beds, locally showing cm-thick lamination, with high porosity values (up to 20%) at outcrop scale. Pores vary from mm to cm in size and lenticular to vuggy in shape with random distribution or crudely aligned along lamination, giving the succession an organic appearance. At microscope scale, these facies are characterised by calcite (micrite and microsparite) with a vacuolated texture, and rarely dolomicrite with a complex porosity network locally obliterated by calcite crystals (Fig. 6G). Contrastingly, dolomicrite-microsparite crust microfacies are less abundant and are characterised by a fine lamination due to the alternation of dolomicrite thin layers, dark in colour, and light colour microsparite layers of calcite crystals that can reach 1.5 mm size (Fig. 6H). A thin interval of dolostones (<1 m) is encountered in the middle part of this dm-thick limestone dominated succession. Macrofabrics in the lower part of the section appear comparable to coated reed fabrics observed in travertines with fibrous crystalline fabrics in steeper beds reminiscent of terrace wall or waterfall deposits (i.e. Guo and Riding, 1998).

The distal part of the geobody (Fig. 6I), out of the logged section and towards the transition between the Upper Cangulo unit and the Upper Tumbalunda Formation, is made of meter-thick laminated and non-laminated clotted dolostones interbedded with the siliciclastic deposits of the Upper Tumbalunda Fm. Locally, these dolostones show a high content in exotic components such as feldspar and quartz grains.

4.1.5. Upper Tumbalunda Fm

The youngest Pre-Salt deposits cropping out in Cangulo palaeovalley correspond to the 40-m-thick clastic dominated Upper Tumbalunda Fm (Fig. 3). The base of this formation is interbedded with the distal part of the Upper Cangulo unit, and progressively overlaps and oversteps both the Upper and Lower Cangulo units (Fig. 7A).

The Upper Tumbalunda Fm. shows a roughly fining upwards trend, ranging from coarse grained sandstones including dm-thick intervals of conglomerates to a dominant coarse-to-fine grain yellow sandstone succession in the upper part (Fig. 7B). Locally, two types of carbonate beds are included in the succession: i) thin laminated cm-thick carbonates beds with smooth domal shape (Fig. 7C); and ii) cross-bedded calcareous sandstones composed of medium grain size with outsized grains locally including large amount of dwelling ichnofabrics (? *Ophiomorpha*) (Fig. 7D and E).

The Upper Tumbalunda Fm. is directly overlain by the Gaio Fm. and Giraul Fm. in the Cangulo region, Both of them being post-salt Albian aged sedimentary units (Fig. 7A). The contact is locally associated with some very steep bedding dips, faults and folds. The top of the Tumbalunda Fm. corresponds to the top of the pre-salt, equivalent to the time of deposition of the evaporites of the Bambata Fm., which is not preserved in Cangulo palaeovalley, but well exposed directly above the Upper Tumbalunda Fm north and south of Cangulo and in other palaeovalleys onshore Namibe Basin (Gindre-Chanu et al., 2015, 2016; Sharp et al., 2016). These data and observations indicate that the Bambata Fm. has likely been removed (dissolved?) in the Cangulo palaeovalley section, and are in keeping with regional mapping in the Namibe Basin, where the Bambata Fm evaporites are typically mapped as patchy erosional remnants of a once extensive evaporite body (Gindre-Chanu et al., 2015; Swart et al., 2016). Partial to full evaporite removal is most commonly observed along the line of palaeovalleys and modern river valleys, for example as seen in the Catumbela, Bentiaba, Chapeau Armado, Ponte Negra, Paimbo and Maraquita regions. This likely relates to greater freshwater discharge and evaporite dissolution along the palaeovalleys (Gindre-Chanu et al., 2015).

4.2. Petrology and geochemistry of depositional and diagenetic phases

Based on the spatial and stratigraphic distribution, petrographic characteristics, and elemental and isotopic composition, both depositional and diagenetic phases have been identified and grouped in 6 main clusters (detailed database included as supplementary material, Tables 2 and 3appsec1). Based on cross-cutting relationships, both at outcrop and in thin section, we established the relative chronology of the diagenetic products observed in the studied units, using their time of deposition as

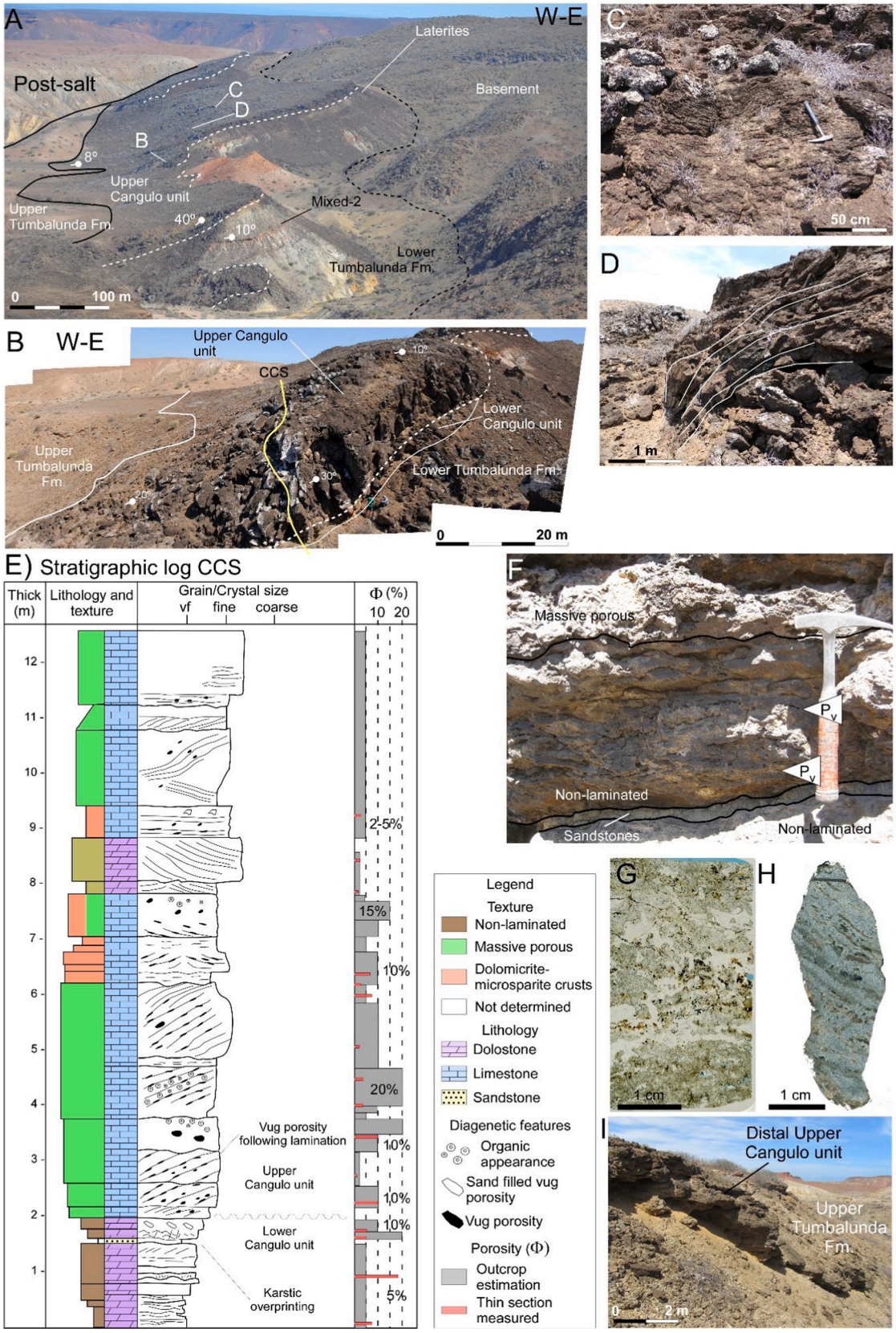

Fig. 6. A and B) Panoramas showing the spatial distribution and large-scale geometry¡ of unconnected bodies of the Upper Cangulo unit. Note the basal erosive character (white dashed line). C and D) Detail outcrop images of special bed morphologies within Upper Cangulo unit. See text in section 4.1.4 for details. E) Stratigraphic log CCS used as a reference log for the Upper Cangulo unit geobodies. The lowermost part corresponds to the unconformable transition between the Lower and Upper Cangulo units (see detail outcrop image in F). G and H) Thin section and sample images showing the main characteristics of massive porous and dolomicrite-microsparite crust textures respectively. I) Outcrop image of the distal part of Upper Cangulo geobodies, where they transition to clastic deposits of Upper Tumbalunda Fm.

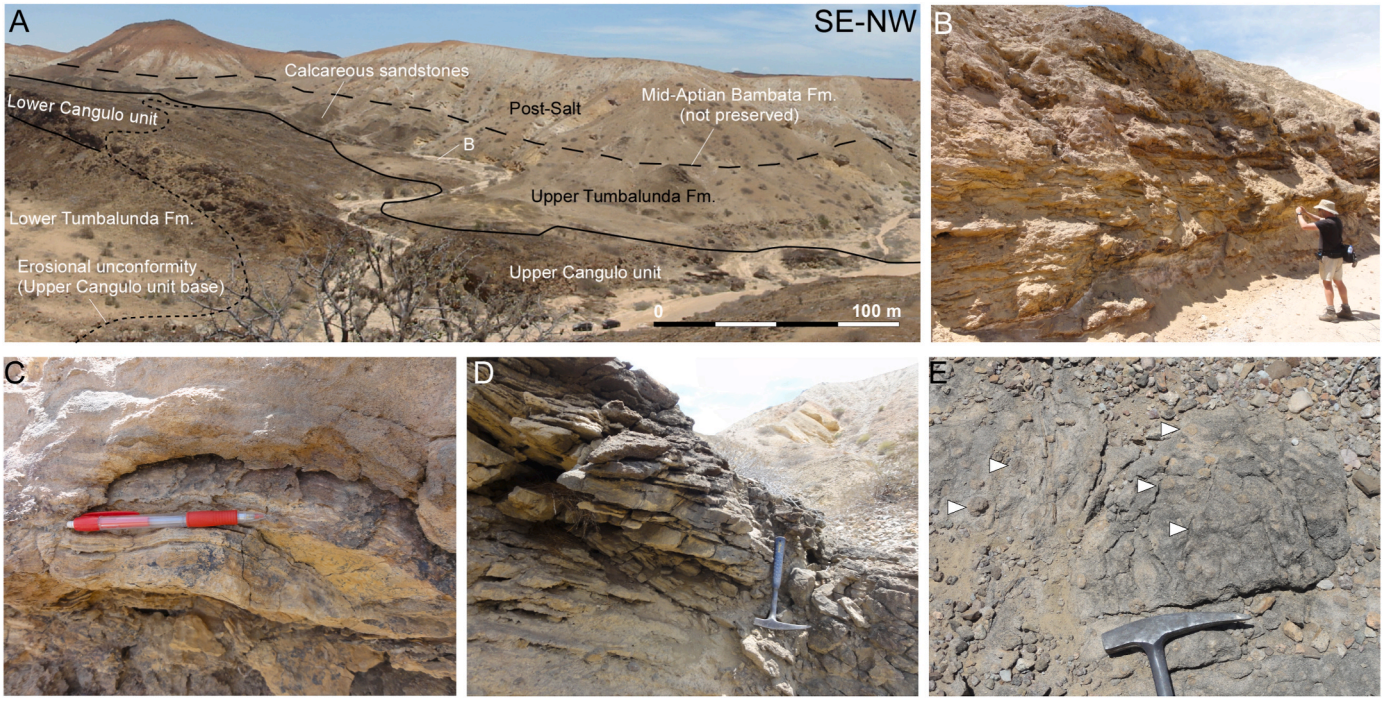

Fig. 7. A) Panorama showing the transition from the Upper Cangulo unit to the Upper Tumbalunda Fm. Note the unconformities at base of Upper Cangulo unit and Post-Salt units. B) Outcrop image showing the alternance of clastic rich and carbonate rich beds composing the Upper Tumbalunda Fm. Carbonates are characterised by thin-laminated beds with domal shape (C) and cross-bedded calcareous sandstones (D) locally bioturbated (white triangles in image E).

benchmarks for the relative chronology (Fig. 8).

Cluster 1: Replacive dolomite 1 (D1) and dolomite cement (DC1)

Replacive dolomite 1 (D1) replaces limestones of the mixed-2 interval of the Lower Tumbalunda Fm. D1 forms anhedral to subhedral crystals ranging in size from 10 to 100 μm and shows a bright red luminescence (Fig. 9A to C). D1 crystals show a penetrative and non-destructive fabric, preserving lamination. The elemental composition is characterised by Ca and Mg content between $21.2{\cdot}10^4$ and $21.6{\cdot}10^4$ ppm and between $12{\cdot}10^4$ and $12.4{\cdot}10^4$ ppm respectively (Fig. 10). Mn and Fe content are between $6.7{\cdot}10^3$ and $9.6{\cdot}10^3$ ppm and $2.7{\cdot}10^3$ and $4.7{\cdot}10^3$ ppm respectively. D1 yielded $\delta^{18}O$ values of +2.04 to +3.27 $‰_{VPDB}$ and $\delta^{13}C$ values of −1.11 to −0.22$‰_{VPDB}$ (Fig. 11). Dolomite cement (DC1) partially fills the intercrystalline porosity, locally enlarged by dissolution, in D1 crystal mosaics. DC1 forms subhedral

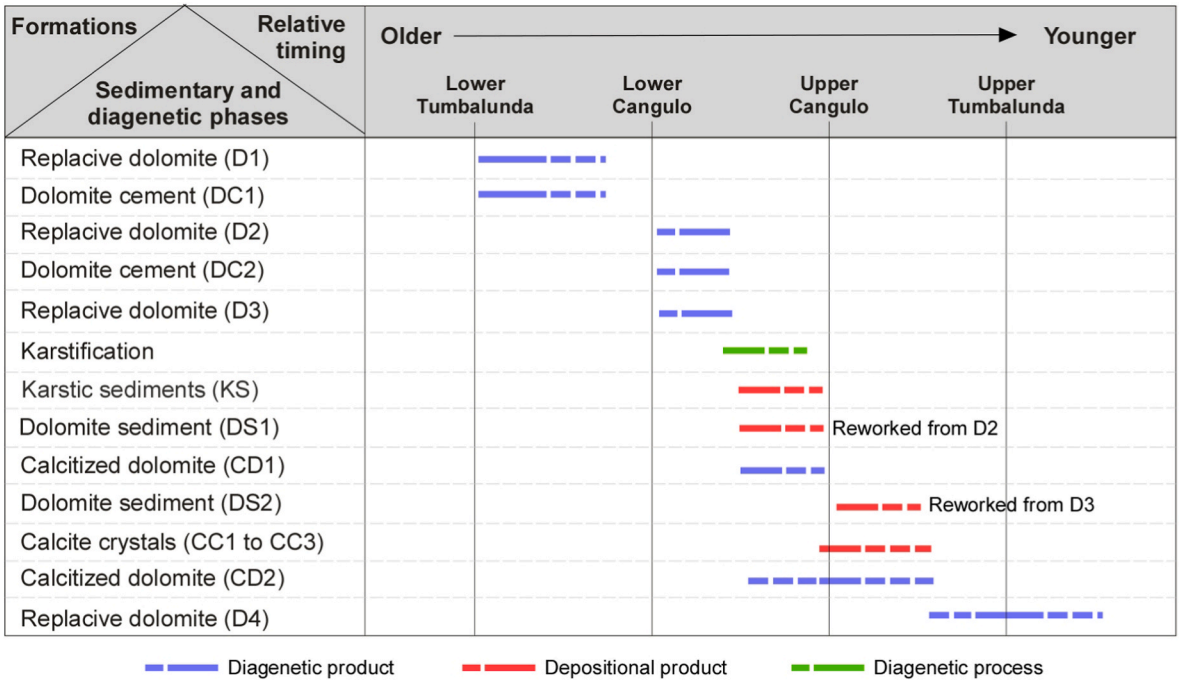

Fig. 8. Relative chronology of the diagenetic and depositional phases encountered in carbonate intervals within the Pre-Salt succession from Cangulo palaeovalley.

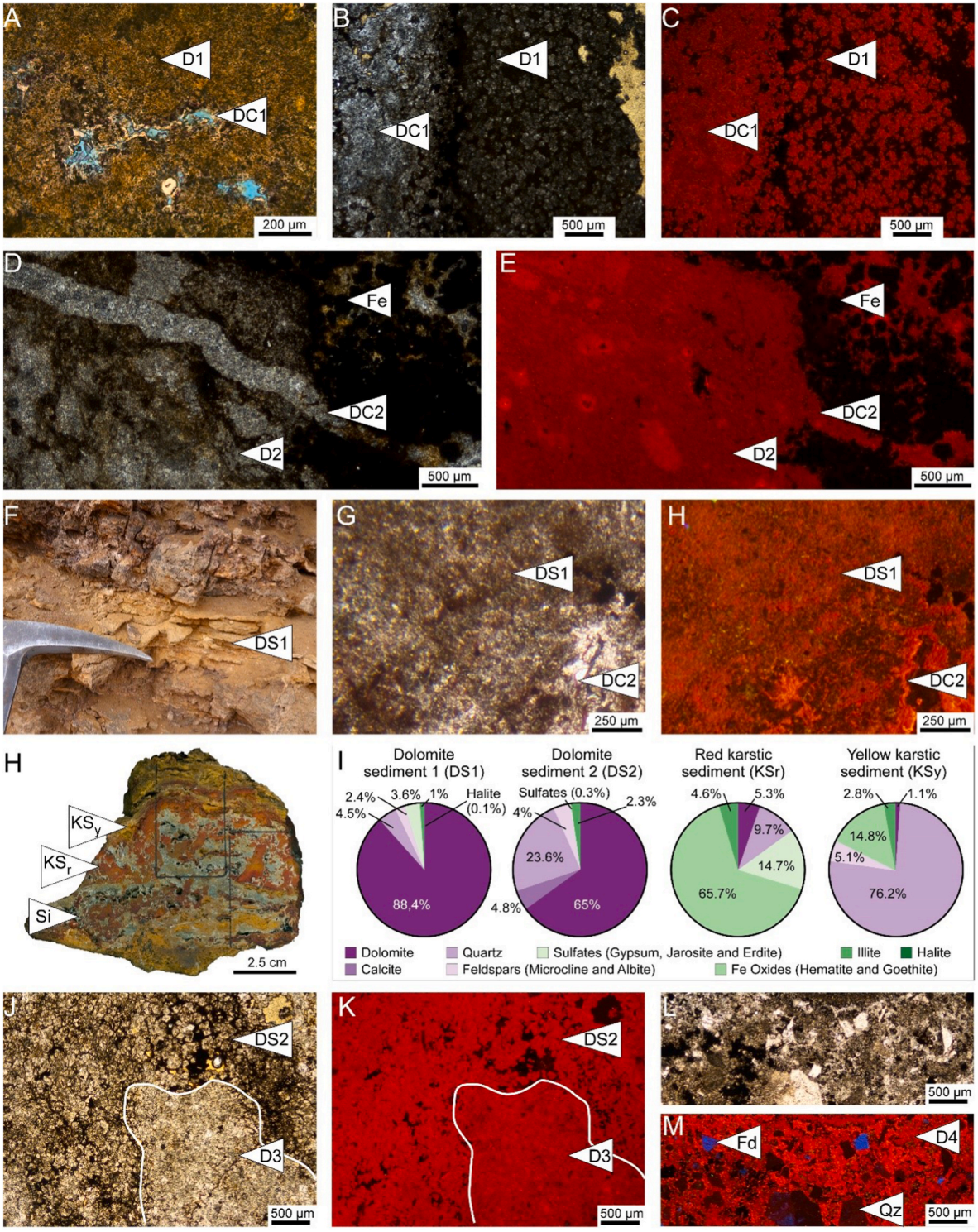

Fig. 9. A, B and C) photomicrographs (plane polarized and cathodoluminescence) of replacive dolomite 1 (D1) and dolomite cement 1 (DC1). D and E) photomicrograph pair (PPL and CCL respectively) showing the main characteristics of replacive dolomite 2 (D2) and dolomite cement 2 (DC2) in pores and fractures, locally encountered with iron-rich crusts (Fe). F) Field image and G and H) photomicrograph pair (PPL and CCL respectively) showing the appearance of dolomite sediment 1 (DS1) and dolomite cement (DC2) in pores. H) Hand sample picture showing two distinctive karstic sediments encountered within the Lower Cangulo unit (red, KSr, and yellow, KSy) accompanied by later silica cement (Si). I) Pie chart showing the X-ray diffraction quantification of the main components of dolomitic sediments (DS1 and DS2) and Karstic sediments (KSr and KSy). J and K) photomicrograph pair (PPL and CCL respectively) showing the appearance of replacive dolomite 3 (D3) and associate dolomitic sediment 2 (DS2). L and M) photomicrograph pair (PPL and CCL respectively) showing the appearance of replacive dolomite 4 (D4) affecting carbonates located in the transition between Upper Cangulo unit and Upper Tumbalunda formation. This caused the high content of detrital components such as quartz (Qz) and feldspar grains (Fd).

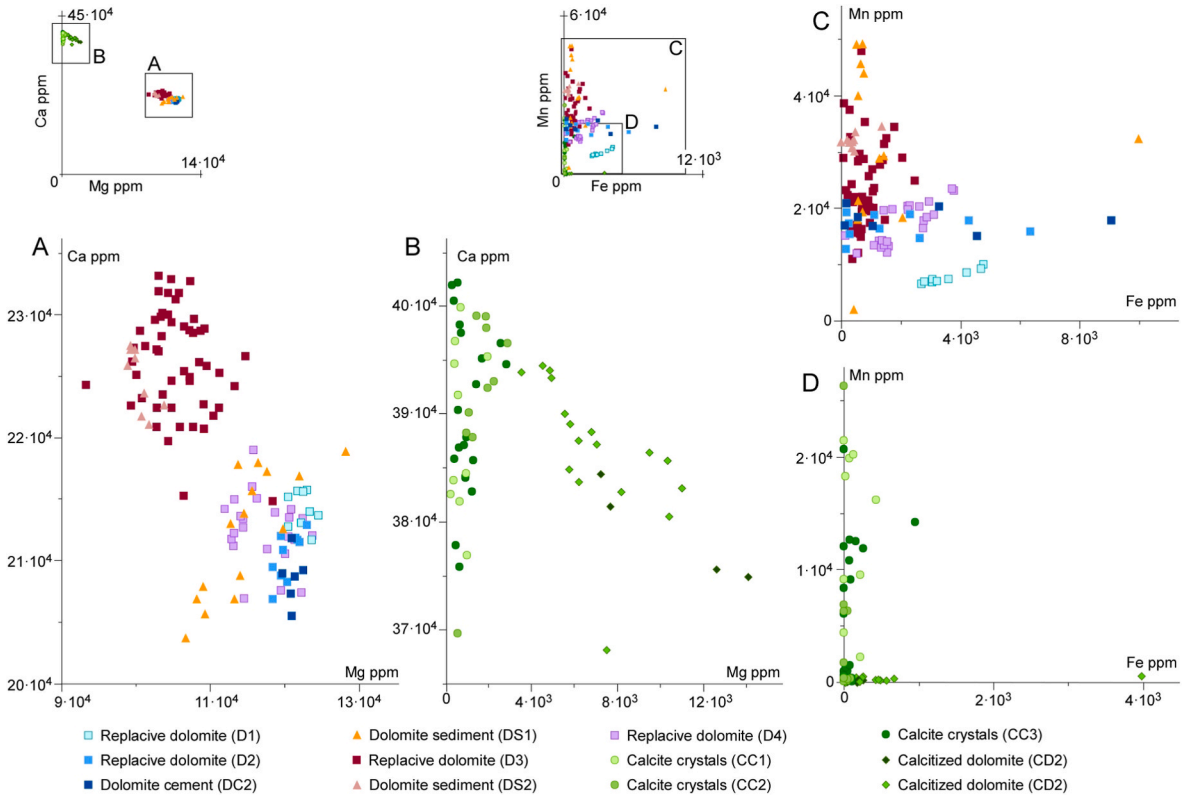

Fig. 10. A to D) elemental composition of dolomite and calcite diagenetic phases in carbonate intervals from Cangulo palaeovalley.

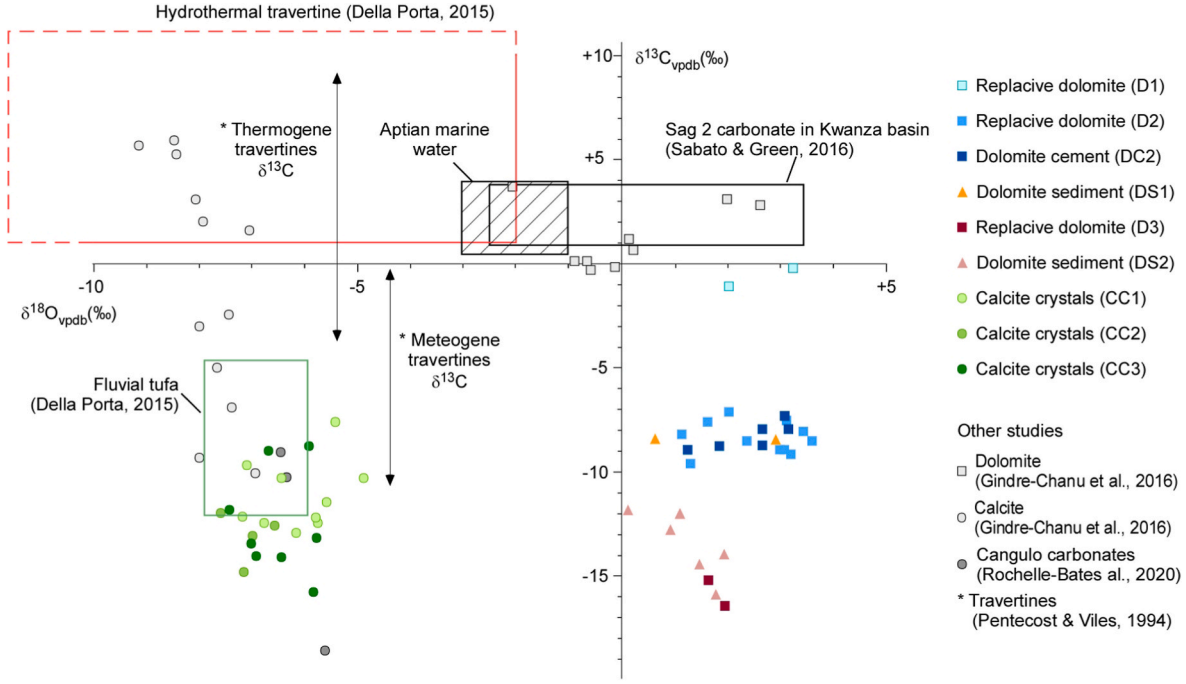

Fig. 11. Oxygen/carbon isotope plot showing the obtained isotopic signature for diagenetic and depositional phases in the Cangulo palaeovalley plotted against data from previous published works.

crystals ranging from 50 to 200 μm in size and show bright red luminescence (Fig. 9A to C).

Cluster 2: Replacive dolomite 2 (D2), dolomite cement 2 (DC2), dolomite sediment 1 (DS1) and karstic sediments (KS)

Replacive dolomite 2 (D2) replaces limestones of the Lower Cangulo unit to form dolostones with penetrative and partially retentive fabric. D2 forms anhedral crystals that range from 10 to 100 μm in size, and shows a red bright luminescence (Fig. 9D and E). Dolomite cement DC2 (DC2) partially fills irregular vugs in D2 crystal mosaics, representing

dissolution-enlarged intercrystalline pores after the replacement, and fractures. DC2 forms subhedral crystals, ranging from 50 to 200 μm in size, and show red bright luminescence (Fig. 9D and E).

Dolomite sediment 1 (DS1) is encountered filling vug and cavernous porosity after DC2 precipitation. DS1 is a yellow colour laminated sediment made of subhedral dolomite crystals that range from 25 to 150 μm in size, and show dull red to orange luminescence (Fig. 9F to H). According to X-ray diffraction, dolomite is accompanied by quartz, feldspars, illite, gypsum and halite (Fig. 8I). In the highly karstified intervals of the Lower Cangulo Fm, DS1 is accompanied by yellowish and reddish karstic sediments (KSy and KSr in Fig. 9H) with distinctive composition; quartz, goethite, dolomite, microcline and illite for the yellow KS, and goethite, hematite, jarosite, gypsum, dolomite, quartz and illite the red KS (Fig. 9I). D2, DC2 and DS1 constituted a well-defined cluster both from elemental and isotopical composition point of view, although elemental composition of DS1 is highly variable compared to D2 and DC2 (Fig. 11). These diagenetic phases have values of $\delta^{18}O$ ranging from +0.64 to +3.64 ‰$_{VPDB}$ and $\delta^{13}C$ from −9.56 to −7.14‰$_{VPDB}$, with elemental composition characterised by Ca and Mg content between $20.4{\cdot}10^4$ and $21.9{\cdot}10^4$ ppm and between $10.7{\cdot}10^4$ and $12.8{\cdot}10^4$ ppm respectively. Mn and Fe content are between $2.1{\cdot}10^3$ and $4.9{\cdot}10^4$ ppm and 128 and $10{\cdot}10^3$ ppm respectively (Fig. 10).

Cluster 3: Replacive dolomite 3 (D3) and dolomite sediment 2 (DS2)

Replacive dolomite 3 (D3) replaces the basal limestones of the succession presented in CCS log (Fig. 6) that appear very near to or just at the contact with the Precambrian basement, corresponding to Lower Cangulo unit D3 forms anhedral to subhedral crystals that range from 10 to 50 μm in size and show red bright luminescence. D3 shows a penetrative and non-destructive fabric (Fig. 9J and K). Dolomite sediment DS2 is encountered as reworked grains accompanied by quartz, illite and microcline in two forms: i) filling vugs in D3 crystal mosaics, thus postdating D3; and ii) included within the depositional facies of the Upper Cangulo unit.

Both D3 and DS2 constitute a very well-defined cluster in terms of isotopic and elemental composition. D3 and DS2 yielded $\delta^{18}O$ from 0.15 to 1.98 ‰$_{VPDB}$ and $\delta^{13}C$ from −16.41 to −11.86 ‰$_{VPDB}$ (Fig. 11), with elemental composition characterised by Ca and Mg content between $21.5{\cdot}10^4$ and $23.3{\cdot}10^4$ ppm and between $9.3{\cdot}10^4$ and $11.8{\cdot}10^4$ ppm

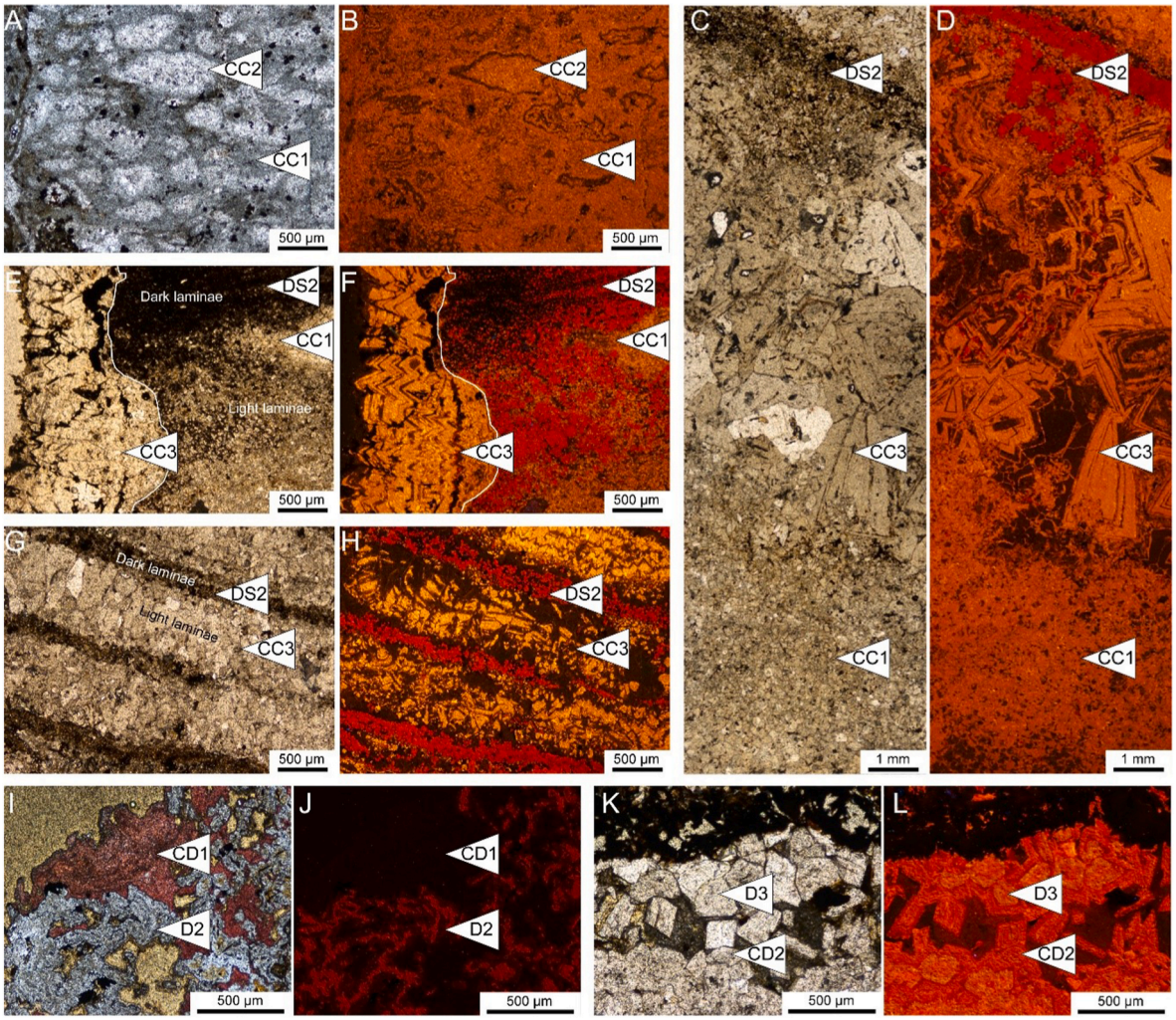

Fig. 12. A and B) photomicrographs (plane polarized and cathodoluminescence respectively) of calcite crystals CC1 and CC2 from massive porous microfacies in the Upper Cangulo unit. C and D) photomicrographs (plane polarized and cathodoluminescence respectively) of calcite crystals CC1 and CC3 and DS2 constituting the laminae alternation of dolomicrite-microsparite microfacies. E and F) photomicrographs (plane polarized and cathodoluminescence respectively) showing calcite crystals CC3 filling vug porosity of a dolomicrite-microsparite microfacies sample. G and H). E and F) photomicrographs (plane polarized and cathodoluminescence respectively) of dolomicrite-microsparite microfacies showing dark laminae constituted by dolomite sediment DS2 and light laminae constituted by calcite crystals CC3. I and J) (plane polarized and cathodoluminescence respectively) of calcitized dolomite CD1 associated to dolomite D2. K and L) (plane polarized and cathodoluminescence respectively) of calcitized dolomite CD2 associated to replacive dolomite D3.

respectively (Fig. 10). Mn and Fe content are between $1.1{\cdot}10^4$ and $4.8{\cdot}10^4$ ppm and below the detection limit and $2.4{\cdot}10^3$ ppm respectively.

Cluster 4: Replacive dolomite 4 (D4)

Replacive dolomite 4 (D4) replace limestones from the distal facies of the Upper Cangulo unit, in the transition between the carbonate beds and the clastic deposits of the Upper Tumbalunda Fm. D4 forms subhedral to euhedral crystals with a red bright luminescence (Fig. 9L and M), locally showing of bright – dull zones. The geochemical composition of D4 is similar to the D2 and other components of cluster 2 that are diagenetic phases affecting Lower Cangulo unit D4 is characterised by Ca and Mg content between $20.7{\cdot}10^4$ and $21.9{\cdot}10^4$ ppm and between $11.2{\cdot}10^4$ and $12.4{\cdot}10^4$ ppm respectively. Mn and Fe content are between $11.9{\cdot}10^3$ and $2.3{\cdot}10^4$ ppm and between 134 and $3.7{\cdot}10^3$respectively (Fig. 10).

Cluster 5: Depositional calcite crystals 1, 2 and 3 (CC1, CC2 and CC3)

Depositional calcite crystals 1, 2 and 3 (CC1, CC2 and CC3) are the major mineral component of the massive porous and dolomicrite-microsparite microfacies of the Upper Cangulo unit CC1 is constitute by micrite to microsparite with a bright orange luminescence that constitutes the frame of the massive porous facies (Fig. 12A and B) and light laminae of the dolomicrite-microsparite microfacies (Fig. 12C to F). CC2, which fills pores of the massive porous microfacies, forms euhedral and translucent crystals featuring drusy geometry and ranging from 50 to 250 μm in size with non to orange dull zoned luminescence (Fig. 12A and B). Finally, CC3 is encountered both as light laminae of the dolomicrite-microsparite microfacies and as cement partially occluding porosity (Fig. 12C to H). CC3 forms euhedral to subhedral translucent crystal ranging from 100 to 500 μm in size and featuring drusy to blocky geometry. CC3 shows a non-to yellow-bright zoned luminescence.

These three calcites define an isotopically distinctive cluster characterised by an isotopic composition very depleted in $\delta^{18}O$ compared to other phases (−7.58 to −4.87 $‰_{VPDB}$ in Fig. 11) and similar $\delta^{13}C$ values (−15.83 to −7.64 $‰_{VPDB}$ in Fig. 11). Their elemental composition is characterised by Ca and Mg content between $37{\cdot}10^4$ and $40.1{\cdot}10^4$ ppm and between below detection limit and $2.7{\cdot}10^3$ ppm respectively. Mn and Fe content are between below the detection limit and $2.6{\cdot}10^4$ ppm, and between below the detection limit and $1{\cdot}10^3$ ppm respectively (Fig. 10).

Cluster 6: Calcitized dolomite 1 and 2 (CD1 and CD2)

Calcitized dolomite 1 (CD1) appears rimming vugs in dolostones forming highly karstified intervals of the Lower Cangulo unit, thus postdating D2 and DC2 (Fig. 12I and J). CD1 forms anhedric crystals ranging from 75 to 150 μm in size and are non-luminescent. Contrarily to CD1, calcitized dolomite 2 (CD2) appears rimming dolomite crystals within the dolomitic sediment DS2 of the Upper Cangulo unit, thus postdating DS2 (Fig. 12K and L). CD2 forms subhedral to euhedral crystals with a red luminescence. CD1 and CD2 have distinctive elemental composition, being CD1 richer in Mg content and depleted in Ca content compared to CD2. CD1 Mg and Ca content range from $7.2{\cdot}10^3$ to $1.4{\cdot}10^4$ ppm and from $37.5{\cdot}10^4$ to $38.4{\cdot}10^4$ ppm, respectively. CD2 Mg and Ca content range from $3.5{\cdot}10^3$ to $1.1{\cdot}10^4$ ppm and from $36.8{\cdot}10^4$ to $39.4{\cdot}10^4$, respectively (Fig. 10). CD1 is depleted in Fe content (between below detection limit and 228 ppm) respect to CD2 (between below detection limit and 683 ppm, with an outlier value of $3.9{\cdot}10^3$ ppm). Both CD1 and CD2 show very low Mn content, below detection limit, with only few analysis points from CD2 not higher than 470 ppm (Fig. 10).

5. Discussion

5.1. Re-interpreting the pre-salt carbonates of the Namibe Basin

Pre-salt carbonates onshore Namibe Basin were interpreted as travertine, tufa and waterlain lacustrine or transitional marine deposits constituting a single lithostratigraphic unit informally named the Cangulo Fm. (Gindre-Chanu et al., 2016; Rochelle-Bates et al., 2020; Sharp et al., 2012). The Cangulo Formation was placed as developed predominantly stratigraphically below the Tumbalunda Formation, typically observed sitting directly on Precambrian basement or igneous units of the Etendeka/Bero volcanics, indeed as it does north and south of Cangulo palaeovalley. The Cangulo Formation however was also described as having complex interfingering relationships with clastics of the Tumbalunda Formation in a number of sections, in particular in the vicinity of palaeovalleys (eg Chapeau Armado, Ponte Negra, Piambo, Bero and Cangulo), and comprising both clear travertine geobodies and thinner water-lain bedded carbonates of uncertain lacustrine to marginal marine microbial affinities (Sharp et al., 2016). The Cangulo palaeovalley section was identified as a well exposed location where the complex Tumbalunda-Cangulo interfingering relationships could be further resolved. New sedimentological, petrological, and geochemical data from Cangulo palaeovalley presented here now indicate that i) the Cangulo Formation should in fact be divided into at least two distinct units that are separated by a major sequence boundary (Lower and Upper Cangulo units), and ii) that the Upper Cangulo unit travertines are younger than previously thought. Several lines of evidence support this new interpretation as described in the following paragraphs.

Sharp et al. (2012) described the Cangulo Fm. as a series of carbonate bodies that typically occur lying directly on top of the Precambrian basement or Bero Volcanic Complex. The Cangulo Fm carbonates were locally described as interbedded with clastics of the Tumbalunda Fm, particularly within palaeovalleys, but regional mapping indicated that Cangulo Fm carbonates were typically the first sag units deposited on basement and Bero Volcanics in the Namibe Basin, and thus likely predominantly older than the overlying several hundred-meter-thick fining upwards "transgressive" succession of the Tumbalunda Fm. (Fig. 2B). However, new field observations from within the Cangulo palaeovalley show that isolated carbonate bodies (now defined as the Upper Cangulo unit) are located in a higher stratigraphic position than originally documented and in fact occur at the base of the uppermost Tumbalunda Fm (Fig. 3B). The stratigraphic juxtaposition of the two carbonate units observed in Cangulo palaeovalley indicates that both Lower and Upper Cangulo units are younger than previously assumed and would probably be time equivalent to the *Lower evaporite unit* defined by Gindre-Chanu et al. (2016). These authors described the *Lower evaporite unit* as a series of carbonate and evaporite intervals deposited in local sabkha and mud flats developed within a tidal dominantly clastic succession. The base of the unit is typically marked by a thin but laterally extensive remnant evaporite horizon. In the type logged section in northern Namibe (Cajanjamba and Tumbalunda valleys, Gindre-Chanu et al., 2016), the interval above the *Lower evaporite unit* is characterised by classic tidal to evaporitic coastal sabkha facies and has a clear gradational and depositional contact to the overlying main Bambata Fm. evaporites. A similar situation is evident in the onshore Benguela and southern Kwanza basins (Equinor, 2011; Sharp et al., 2016).

It therefore follows, that in agreement with the above mentioned paleogeographic setting, our new results indicate that the Lower Cangulo unit carbonates were deposited in a transitional to marginal marine tidal-influenced environment. Field observations supporting this interpretation are: i) the carbonates are interbedded within the Tumbalunda Fm. with the underlying and overlying clastic intervals showing abundant tide-related sedimentary structures such as herringbone cross-bedding, mud-flake rip-ups and bi-directional current ripples in association with grazing and dwelling icnofabrics, including bivalve resting traces (Fig. 4); ii) the occurrence of tepee structures, low relief dome

shaped beds, fenestral porosity and planar to wavy fine-laminated facies (Fig. 5), typically related to microbial- and algal-induced carbonate deposition in intertidal or marginal marine zones (Lasemi et al., 2012; Matysik, 2016; Shinn et al., 1983; Wright, 1990); iii) the subparallel, fairly continuous stratal pattern of the Lower Cangulo unit compared to the stratal pattern of the Upper Cangulo unit (Fig. 4) indicates deposition in a flat topography such as tidal flats to coastal sabkha (Rankey and Berkeley, 2012); and iv) the presence of pseudomorphs of evaporites (probably gypsum or glauberite based on their morphology, Fig. 5H), suggesting a saline environment under a relatively hot climate (i.e., with a high rate of evaporation) that favoured the growth of evaporite minerals within carbonate mud (Salvany et al., 2007). Halite and gypsum pseudomorphs have also been documented in equivalent intervals in Benguela and Gaio regions (Gindre-Chanu et al., 2016). In this regard, the general lack of biota along the entire Lower Cangulo unit succession could be associated with these arid and saline environmental conditions (Mercedes-Martín et al., 2014; Tucker, 1991), which fits well with the regional arid climate zone prevailing during Aptian times in the area (Chumakov, 1995; Hay and Floegel, 2012).

An evaporative depositional setting for the Lower Cangulo unit is also suggested by the early diagenetic replacive dolomite (D2 and D3) and dolomite cement (DC2) that overprint the depositional carbonate texture (Fig. 8). The positive $\delta^{18}O_{vpdb}$ signature of D2, DC2 and D3 dolomites (+1 and + 4‰, Fig. 11) are slightly heavier than the expected values for dolomites precipitated from an Aptian marine fluid. The oxygen isotopic signature of those marine-related Aptian dolomites would range between −1 and +3‰, applying the correction factor of $\Delta^{18}O_{Dol-Calcite}$ between +2 and + 4‰ (Arenas et al., 1997; Budd, 1997; Geske et al., 2012) to the −3 and −1‰ $\delta^{18}O_{vpdb}$ signature of Aptian (early Cretaceous) marine carbonates (Ferreri et al., 1997; Veizer et al., 1999). The enrichment on heavy oxygen isotopes is attributed to the precipitation from evaporated marine water under a high rate of evaporation (Fig. 11). The obtained oxygen values for the Lower Cangulo dolostones are consistent with those rates reported for other marine-related dolostones from the Upper Sag succession onshore Namibe Basin (Gindre-Chanu et al., 2016) and hypersaline lacustrine carbonates offshore Kwanza Basin (Sabato-Ceraldi and Green, 2016).

Contrarily to the oxygen signature, the carbon isotopic values of Lower Cangulo dolostones (D2, DC2 and D3) is highly depleted (−6 to −16‰; Fig. 11) compared with other upper sag carbonates from the South Atlantic basins (Gindre-Chanu et al., 2016; Sabato-Ceraldi and Green, 2016). This shift is interpreted to result from the interaction of Aptian evaporated marine water with fluids derived from: i) microbial sulphate reduction (Mazzullo, 2000; Preto et al., 2015), ii) oxidation of organic matter (Moore, 2001) and/or iii) interaction with meteoric fluids (Bustillo et al., 2017). All three processes are feasible in the interpreted sabkha and tidal flat depositional setting and they potentially coexisted in the Cangulo palaeovalley. However, the Lower Cangulo dolostones located near the basement, and just beneath the Upper Cangulo unit (Fig. 6), show more depleted $\delta^{13}C_{vpdb}$ (from −12 to −16‰, D3) than equivalent dolostones located in distal areas (from −7 to −10‰, D2 and DC2). This spatial distribution suggests that the interaction between evaporated marine water and meteoric fluids would be the prevailing dolomitization mechanism in areas close to the Cangulo palaeovalley basement. This interpretation is also supported by Mg/Ca variation in D2, DC2 and D3 dolomites that follows the same trend; Mg/Ca ratio decrease in areas near the basement (D3) in comparison with distal ones (D2 and DC2, Fig. 10), likely resulting from a higher influence of meteoric water (Folk and Land, 1975; Hayes and Boles, 1993).

Results indicate that Upper Cangulo unit was deposited after the exposure and partial erosion of the Lower Cangulo unit and Lower Tumbalunda Fm., as recorded by the erosional unconformity between both carbonate units (Figs. 6 and 13). Contrary to the Lower Cangulo, field data indicate that the Upper Cangulo carbonates, dominantly limestones, correspond to a travertine system characterised by isolated bodies attached to the basement and deposited following a palaeorelief caused by erosion most probably linked to a significant regression. We use here the term travertine in a broad sense representing fresh water (non-marine) subaerial carbonates as Upper Cangulo carbonates include characteristics of both travertine and tufa systems (e.g., regular bedded fabric from travertines or dominantly micritic to microsparitic crystal size from tufas) listed in Capezzuoli et al. (2014).

Following the morphological classification of travertine and tufa complexes (Della Porta, 2015; Luo et al., 2021b, 2021zkul et al., 2002), the predominant depositional environment in the Cangulo palaeovalley is slope, including smooth slopes (perched?) and terraced slopes with local waterfalls and cascades with ponds (Figs. 6 and 13). Moreover, pools have been also identified south of the main Cangulo palaeovalley (Fig. 13) and are spectacularly well exposed in the Chapeau Armado area to the north of Cangulo (Sharp et al., 2012; Rochelle Bates et al., 2020). Field and petrographic data shows that the Upper Cangulo travertines are dominantly made of massive porous facies accompanied by dolomicrite-microsparite crusts (Fig. 6). The origin of the massive porous travertines is unclear but, based on their organic appearance at outcrop, they resemble the "*reed travertine lithotype*" resulting from the precipitation of calcite due to the presence of plant stems and roots, typically encountered in the low energy environments of terraces and pools (Della Porta et al., 2017; Guo and Riding, 1998, 1998zkul et al., 2002). Moreover, the vacuolated texture observed at outcrop and microscope scales in the massive porous facies (Fig. 12) can also be compared to "*coated bubble lithotype*" that is associated with stagnant or low-energy flow conditions in pools and ponds of terraced slope environments (Chafetz and Folk, 1984; Della Porta et al., 2017; Erthal et al., 2017; Gandin and Capezzuoli, 2014). This vacuolated (e.g., bubbles) texture is interpreted to result from agitated waters or microbial metabolic activity. Either if the massive porous microfacies would correspond to the reed or to the bubble lithotype, their origin is related to a depositional setting with low energy water flow that fits well with the very smooth morphology of the travertine bodies observed in the Cangulo palaeovalley. The aforementioned interpretation of massive porous microfacies would also apply in nearby localities, eg Chapeau Armado, Ponte Negra, Piambo, Maraquita and Bero areas, where other Upper Cangulo sections consist of dominant massive porous microfacies associated to pool fill and cascade facies.

Dolomicrite-microsparite crusts are characterised by an alternation of thin layers of dark coloured fine crystalline dolomite (dolomicrite), and light colour layers of fine calcite crystals (microsparite) (Figs. 6H, 12G and H). Dolomite has been rarely found in tufa or travertine systems (exemples in Barnes and O'Neil, 1971; Folk, 1994; Kitano, 1963; Renaut and Jones, 1997). However, Özkul et al. (2013) described mm-scale layers of detrital dolomite laying between calcite laminae in carbonates deposits from Denizli Basin (Turkey). We invoke this origin for the dolomite laminae observed in the Upper Cangulo bodies. According to petrographic observations, the identified dolomite within crust facies is not a replacive or cementation product but a dolomitic sediment (DS2, Fig. 12). In addition, the elemental and isotopic composition of this dolomitic sediment (DS2 in Figs. 10 and 11) is comparable to the geochemical signature of the underlying dolostone beds of the Lower Cangulo unit (D3 in Figs. 10 and 11). This points to the partial erosion of Lower Cangulo unit as a source of the dolomitic sediment incorporated in the dolomicrite-microsparite crust beds. Erosion of basal dolostone and incorporation of dolomitic sediment to the systems suggest a relatively energetic environment that would agree with the presence of the crystalline crust facies. Although not equivalent, we can compare the crystalline facies of dolomicrite-microsparite crust to the "*crystalline crust lithotype*" or "*Micrite-Microsparite crust boundstones*" defined in travertine and tufa complexes (Della Porta et al., 2017; Guo and Riding, 1998; Luo et al., 2021a, 2021zkul et al., 2002). Those facies are typically associated with abiotic processes under an agitated and rapidly flowing water that occurred in slope settings (Della Porta et al., 2017; Erthal et al., 2017; Guo and Riding, 1998). Tufa and travertine complexes are

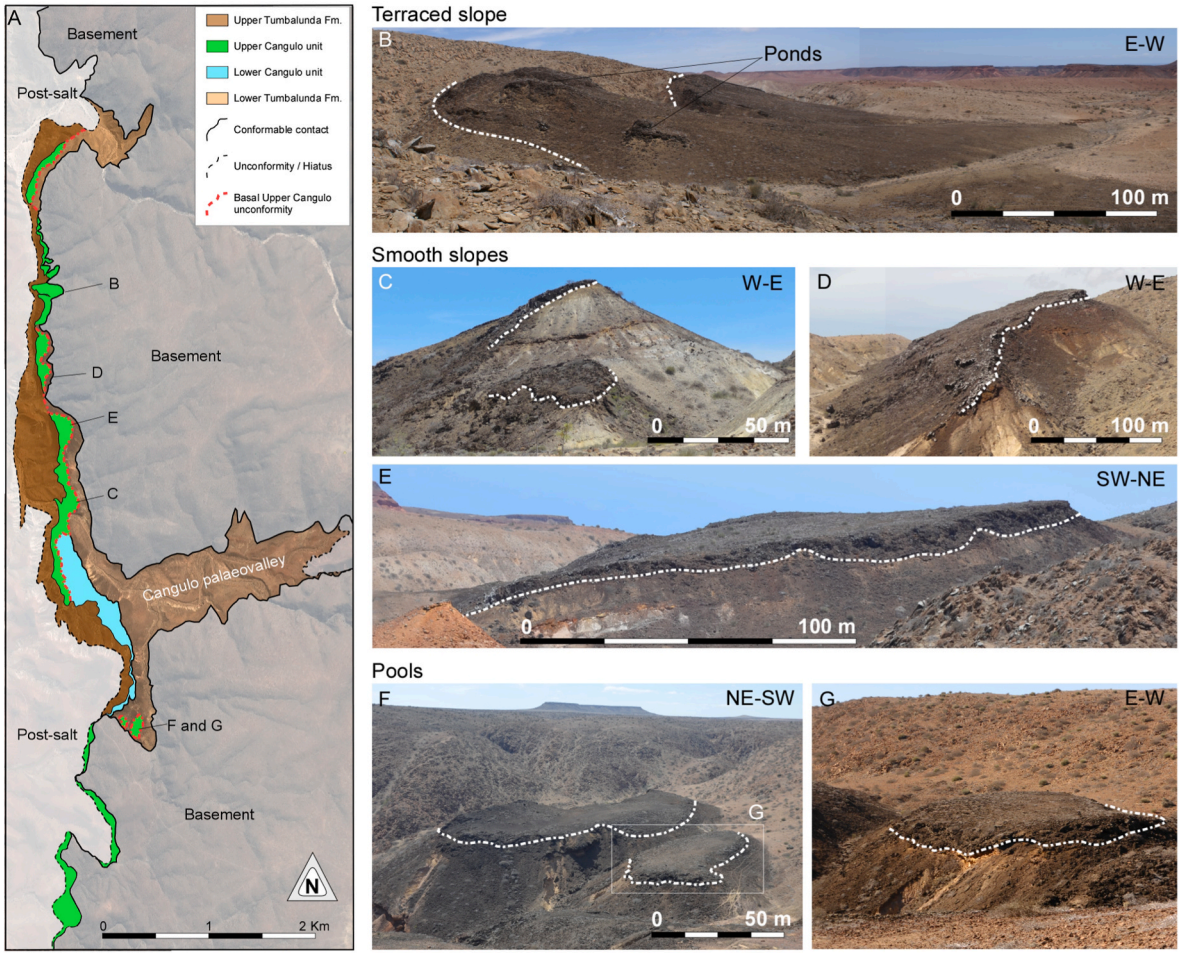

Fig. 13. Morphological characterization of travertine systems corresponding to the Upper Cangulo Unit. A) Geological map with Pre-Salt units differentiated showing the location of some examples of the travertine complex in the Cangulo palaeovalley. B) Panorama showing the geometry of a terraced slope characterised by the presence of ponds associated with subhorizontal beds. C, D and E) Representative images of travertines with a morphology of smooth slopes laying on top of the erosional unconformity (white dashed lines). F and G) Images of two well-developed pools with subhorizontal internal bedding and circular shapes.

very dynamic, being waterflow velocity highly variable through space and time (Gandin and Capezzuoli, 2008; Guo and Riding, 1998; Rainey and Jones, 2009). In the Cangulo palaeovalley, this is recorded by the alternation of the low-energy massive porous limestones and the rapid flow dolomicrite-microsparite crust beds.

Oxygen and carbon isotope values of the three calcite types forming the Upper Cangulo travertines (CC1, CC2 and CC3) range between −7.58 and −4.87 ‰$_{VPDB}$ and −15.83 and −7.64 ‰$_{VPDB}$, respectively (see Fig. 11). The reported range displays a distribution consistent with the meteoric calcite line reported by Lohmann (1988) and is similar to the reported isotopic signature in fluvial tufa characterised by cool or ambient temperature fluids (Andrews, 2006; Della Porta, 2015; Gandin and Capezzuoli, 2008; Zeng et al., 2021) as well as with values for the meteogene travertines defined by Pentecost and Viles (1994). The carbon isotope values of calcites CC1, CC2 and CC3 are clearly distinctive than that reported for hydrothermal/high temperature travertine complexes or thermogene travertines that commonly show a more positive carbon signature (see hydrothermal and thermogene fields in Fig. 11, extracted from Della Porta, 2015; and reference therein; Pentecost and Viles, 1994). Using a numerical approach for $\delta^{18}O_{vpdb}$ of Upper Cangulo samples, and applying fractionation curves of calcite (Friedman and O'Neil, 1977; Salardon et al., 2017) for a temperature lower than 30 °C (i.e. low temperature travertine systems), the resulting $\delta^{18}O_{smow}$ of the parent fluid would rest between −10 and −3‰, which is a typical signature of meteoric or slightly evaporated meteoric fluids. Thus, a low temperature fluid with meteoric signature is envisaged as the most plausible origin of the travertine complexes in the Cangulo palaeovalley. According to Schröder et al. (2016), no freshwater travertine systems have been previously reported in the Cretaceous in the South Atlantic. Consequently, the presented results make the Upper Cangulo unit the first reported evidence of this type of non-marine carbonate system on the African margin of the South Atlantic.

The reported outcrop geomorphology (pools, terraces, slopes) and isotopic signature in the Upper Cangulo travertine complex is comparable to those reported in a travertine geobody from the Chapeau-Armado outcrop located 12 Km to the north of Cangulo palaeovalley. Rochelle-Bates et al. (2020) reported isotopic values of calcite veins and recrystallised host-rock very similar to the ones in Cangulo palaeovalley. However, the diagenetically altered travertine from the Chapeau-Armado area record a much later diagenetic story (84 Ma) linked to different fluids than that of the depositional or early diagenetic ones interpreted in Cangulo palaeovalley. In the Chapeau-Armado area, field and petrographic data record overpressure fracturing, calcite and dolomite cements accompanied with the emplacement of bitumen occurring due to the circulation of high temperature volcanic-related fluids adjacent to a major nepheline-basanite igneous plug. Those diagenetic phases have not been identified in the Upper Cangulo unit of Cangulo palaeovalley, likely due to the absence of a comparable igneous plug as developed in the Chapeau Armado area.

All the low temperature travertine bodies presented in the present work are located over fractured and faulted metasedimentary rocks, whereas elsewhere in the Namibe Basin (eg., Piambo, Maraquita and

Bero region) Cangulo Fm. travertines are developed above igneous rocks of 131–134 Ma ages (Etendeka/Bero vocanics). Younger volcanic-related travertines systems (Coniacian-Santonian) linked to high temperature fluids are reported in other areas of the onshore Namibe Basin (Fiordalisi et al., 2021). Regional mapping in the Namibe and Benguela basins indicate both the Early and Late Cretaceous travertine systems show a clear spatial relationship to fault and fracture systems (Sharp et al., 2016).

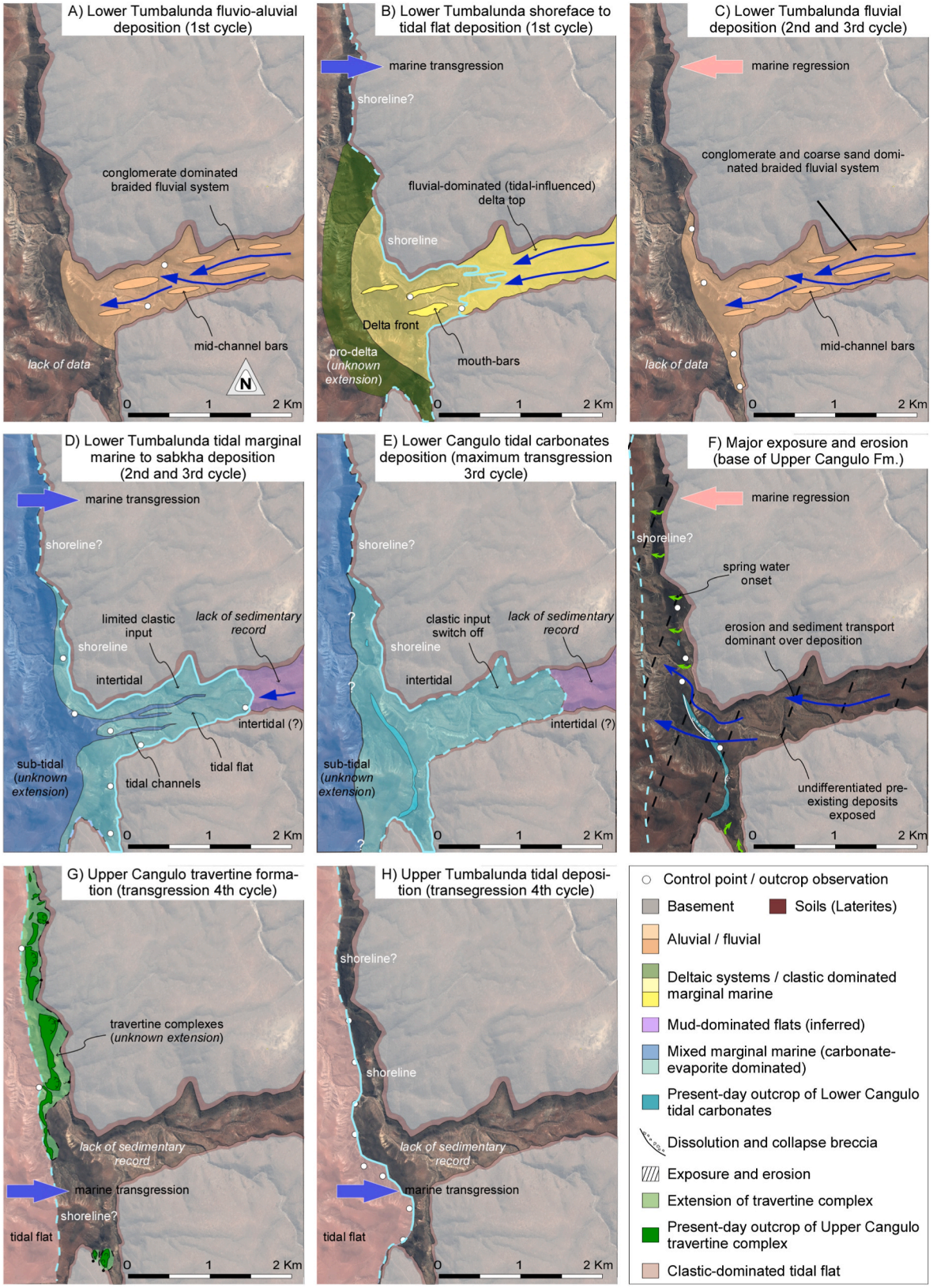

Fig. 14. Palaeogeographic maps showing the distribution of depositional environments along Cangulo palaeovalley during late sag period (Early Aptian).

5.2. Sedimentological and diagenetic evolution of Cangulo palaeovalley

Cangulo palaeovalley represents a key locality that helps to significantly refine understanding of the depositional and palaeohydrological regime that existed during the terminal episodes of the upper sag sequence onshore Namibe Basin, and by extension in the South Atlantic Pre-Salt. Compiled regional, sedimentological, petrographical and geochemical observations and data from the outcropping Pre-Salt succession in Cangulo palaeovalley allows for the first time establishment of a complex depositional and diagenetic evolution for the latest sag South Atlantic pre-salt succession that is summarised in the following paragraphs.

Results from Cangulo palaeovalley allow differentiation of at least three high order transgressive-regressive cycles (T-R) within the upper sag sedimentary succession, with a final transgressive event that is topped by deposition of the Mid-Aptian evaporites of the Bambata Fm. (although this unit is not preserved in the study area, Fig. 3). The first T-R cycle initiates with transgressive deposits of the clastic-dominated basal Lower Tumbalunda Fm., which is interpreted as representing an alluvial to fluvial depositional setting (Fig. 14A and Fig. 15A) dominated by westward flowing ephemeral braided rivers (Sharp et al., 2016). The most transgressive deposits of the first cycle are the ones from the central part of the mixed interval-1 (Figs. 4, 14B and 15B), which likely represent marginal marine shoreface to tidal flat sediments. Mixed interval-1 sandstones can be interpreted as deposited in two distinct settings; mouth bar or pro-delta, dominated by outflow/fluvial discharge processes with rare wave reworking (Figs. 14B and 15B). The more heterolithic and silt-sand interbedded facies cut by shallow scours and channels filled with bi-directional cross bedding, ripples (Fig. 4), mud drapes and locally intensive bioturbation are more indicative of a sub-to inter-tidal flat/marginal marine setting (Dalrymple and Choi, 2007; Davis, 2012). The uppermost part of the mixed interval-1 records the onset of the regressive deposits of the first T-R cycle, characterised by a sand-dominated interval that is topped by a channelized and strongly erosive contact that records an abrupt regression.

The second T-R cycle initiates with a succession comprising multistory and laterally stacked channels interpreted as a fluvial system dominated by conglomeratic and coarse sandy sediments that run towards the west according to clast imbrication (Fig. 14C and Fig. Fig. 15A). The most transgressive deposits of the second cycle are

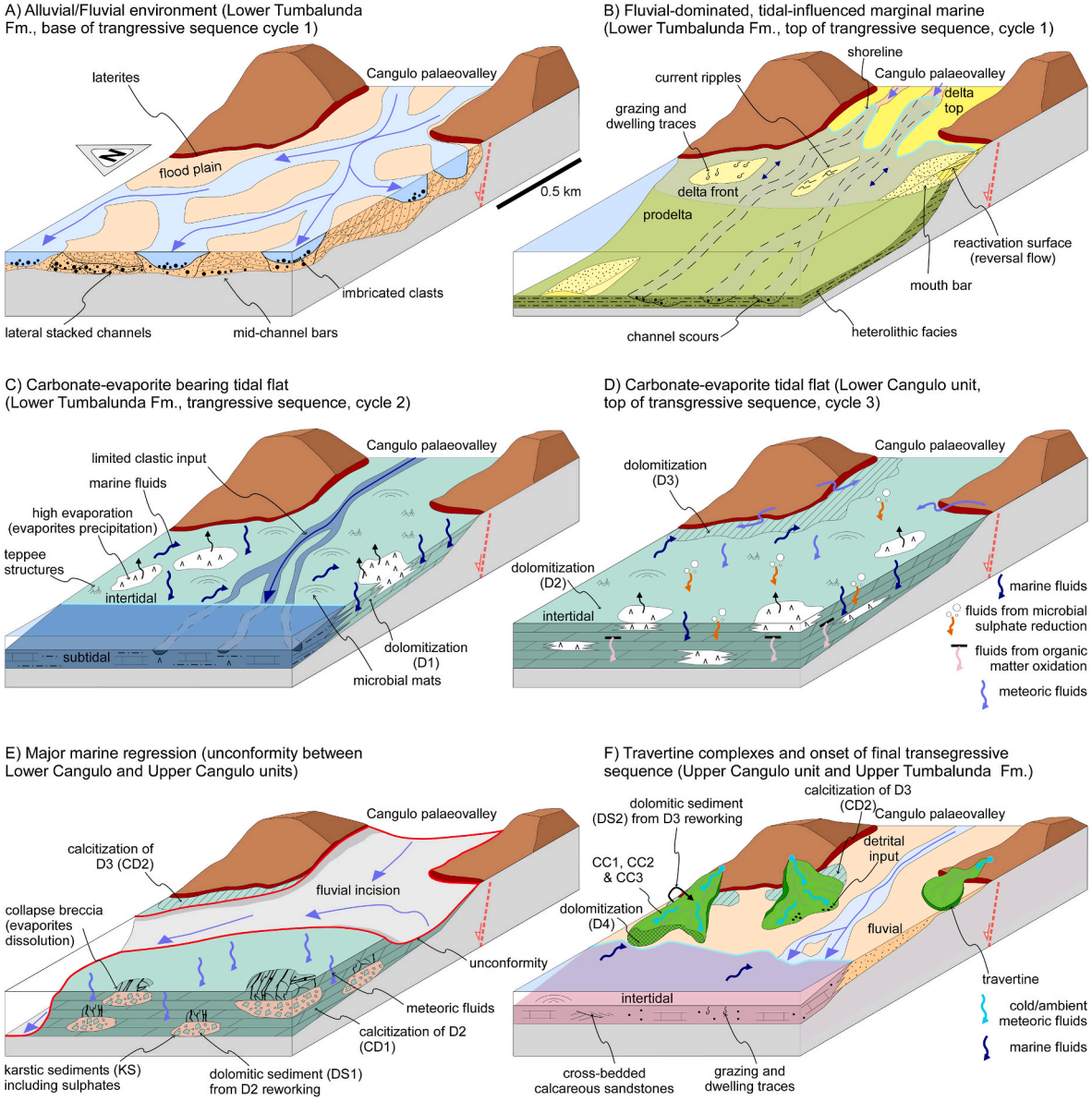

Fig. 15. Block diagrams showing sedimentary system distribution and fluid flow regime in Cangulo palaeovalley during latest sag period (Early Aptian).

made of a mixed clastic-carbonate-evaporitic succession (mixed-2 interval, Fig. 4). Deposition in a tidal marginal marine to coastal sabkha setting is envisaged during this transgression, which was more extensive than the previous one, as the clastic – carbonate interval can be traced more than 1.5 km landward towards the interior of Cangulo palaeovalley (Figs. 14D and 15C). Tidal influence in the clastic dominated periods is recorded by sedimentary structures such as climbing and bi-directional ripples, very well-developed herringbone, tabular to low angle trough cross sets, and truncation/reactivation surfaces (Fig. 4). During the episodic decrease of clastic input precipitation of carbonate and evaporite intervals was favoured, with biogenic carbonates colonizing clastic bedform tops (mixed-2, Fig. 4). The laminar, domal to radial microbial-induced carbonates, encountered in the mixed-2 interval, were replaced soon after deposition by replacive dolomite (D1) and the porosity partially occluded by dolomite cement (DC1). Oxygen isotopic signature of replacive dolomite (D1 in Figs. 11 and 15C) is similar to the expected values for a marine origin (Ferreri et al., 1997; Veizer et al., 1999), with very limited influence of meteoric fluids consistent with a decrease in surface water run-off as suggested by their high Mg/Ca ratio (Folk and Land, 1975; Hayes and Boles, 1993) and low content in Mn (Li et al., 2019). Although direct evidence of evaporite deposition was not found; the sulphur mineral phases found in this interval (gypsum and jarosite >30%, Fig. 3F) suggests the presence of primary depositional sulphates, later dissolved and reprecipitated (Long et al., 1992; Warren, 2016). The regressive deposits of the second T-R cycle comprise a less than 2 m thick sandstone interval capped by a sharp, erosive contact linked to an interpreted rapid regression that marks the end of the cycle.

The third T-R cycle comprises the upper part of the Lower Tumbalunda Fm. and the Lower Cangulo unit. It initiates with a sharp and erosive contact overlaid by a conglomerate-dominated interval interpreted as a consistent westward flowing fluvial system (Fig. 13). Gradational upward transition to a heterolithic succession with distinctive mud drapes, well-developed planar, current, and tabular trough cross bedding, together with common rip-up clasts suggest deposition in a transgressive setting from fluvial to marginal marine tidal flat (Fig. 14D). The most transgressive deposits of the third T-R cycle correspond to the Lower Cangulo carbonates, which are interpreted to represent an arid tidal flat depositional setting with biologically-induced carbonate precipitation (see detailed discussion in section 5.1). The deposition of those carbonates suggests limited clastic input and runoff, and high evaporation rates (Figs. 14E and 15D). The inner part of the Cangulo palaeovalley do not register sediments of this stage as they were later eroded. As detailed in the previous section, analytical data suggests that the Lower Cangulo unit carbonates were dolomitized in close association with the circulation of mixed fluids (marine fluids combined with fluids derived from microbial sulphate reduction, organic matter oxidation and/or meteoric waters). Analytical data indicate that the isotopic signature of the resulting dolomites (Fig. 11) varies depending on the distance from the exposed basement (Fig. 15D).

The regressive part of the third cycle is characterised by the diagenetic overprint of the Lower Cangulo carbonates and the major erosional unconformity at the top of this unit. The Lower Cangulo unit shows well-developed karstic collapse breccia intervals (Fig. 5) characterised by cycles of rubble float breccia (monomictic and heterometric host rock dolostones clasts) transitioning to mosaic and to crackle pack breccia upwards within the cycles. All these characteristics, together with the presence of sulphates in the karstic and dolomitic sediments of the breccia matrix (KS and DS1, Fig. 9I), indicate that the Lower Cangulo unit was originally composed by an alternance of carbonates and evaporites, which were dissolved due to interaction with meteoric waters. These breccias show additional characteristics comparable to the ones reported in other collapse breccia formed by evaporite dissolution such as: i) sharp lower contact of the breccia cycles (Daniels et al., 2020; Swennen et al., 1990), ii) gradual transition into overlying strata (Daniels et al., 2020; Swennen et al., 1990), iii) presence of calcitized dolomite (see calcitized dolomite in Lower Cangulo unit, CD1 in Fig. 11I and J) (Daniels et al., 2020), iv) monomictic heterometric and unsorted clasts originated from the overlying strata (Daniels et al., 2020; Friedman, 1997; Scholle et al., 1993), and v) localised brecciation in limited intervals or zones (Daniels et al., 2020; Friedman, 1997; Scholle et al., 1993; Swennen et al., 1990). The aforementioned authors reported examples of similar processes in the Permian Karstryggen Fm. (Greenland), the Carboniferous (Visean) Belle Roche breccia (Belgium) or the Permian Rocker Fm. (UK). This interpretation agrees with the facies model proposed by Gindre-Chanu et al. (2016) for the later sag onshore Namibe Basin. Based on observations from the South and North Angola margin, these authors interpreted that an extensive shallow sabkha was emplaced in the proximal region of the basin where deposition of inter-layered evaporites and microbialitic carbonates occurred. Therefore, the observations from the Cangulo palaeovalley reported here suggest the occurrence of an equivalent marginal marine depositional setting (i.e., sabkha) in the central part of the onshore Namibe Basin.

The mineralogical composition of the Lower Cangulo breccia matrix suggests that the infiltration of meteoric waters was active at the time of deposition. The matrix of rubble floatbreccias is composed by karstic sediments that include feldspars and quartz that were likely eroded from the Palaeozoic basement and incorporated into the karstic sediments. In this regard, despite iron oxides in karstic sediments being typically associated with insoluble residue after carbonate dissolution, infiltrated meteoric waters that interact with laterites from the altered basement could be an additional/alternative source for iron oxides. Finally, the isotopic and elemental composition of the carbonate fraction in the breccia matrix (dolomitic sediment, DS1) is equal to those of the host rock (D2), suggesting that DS1 may have an origin related to erosion of the host rock during subaerial exposure (Baqués et al., 2013; Travé et al., 2021).

The dissolution of evaporites, dolostone karstification and local erosion of the Lower Cangulo unit is interpreted to be linked with a major relative sea level fall (Kervin and Woods, 2012 and reference therein), and this represent the maximum expression of the regressive tract of the third T-R cycle. Based on the spatial distribution of breccia outcrops and tidal deposits from the innermost part of the Cangulo palaeovalley, the shoreline migration during this regression is estimated to have been at least 1.5 km towards the west (Figs. 14F and 15E). Moreover, this regression was also likely the origin of partial erosion of the siliciclastic deposits of the Lower Tumbalunda Fm. that resulted in the basal unconformity of the Upper Cangulo unit. The stratigraphic position of the unconformity constrains this major regression as intra-Tumbalunda Fm., possibly regionally equivalent to an intra Chela–Cuvo event within the latest upper sag succession (Brownfield and Charpentier, 2006; Burwood, 1999; Marton et al., 2000).

Above the major marine regression, transgressive deposits of the fourth and final T-R cycle are represented initially by deposition of the Upper Cangulo travertines (see details section 5.1). We interpret that the marine regression of the third T-R cycle probably caused changes in the level of the groundwater table that resulted in the onset of freshwater springs along the fractured and faulted basement and the development of travertine complexes. Similar mechanisms are reported in Lake Bogoria by Renaut et al. (2013), where changes in lake level allow the development of thermogene travertines in the so-called Travertine Window.

Upper Cangulo carbonates facies located in the distal parts of the travertine bodies show a high content of exotic components like feldspar and quartz grains, which record the income of detritus probably related to the increase of fluvial activity (Fig. 15F). The predominantly meteoric fluid regime is also recorded by the presence of calcitized dolomite (CD2, Fig. 12K and L) that has been related to the interaction of the dolomite sediment (DS2) of the Upper Cangulo travertines with meteoric waters (Fig. 15F).

The Upper Cangulo travertines change laterally and vertically to

siliciclastic deposits of the Upper Tumbalunda Fm., which progressively onlap the previous deposited units, recording the final transgression and migration of the shoreline landward (Fig. 14G, H and 15F). Analysis of partial dolomitized distal travertine beds (D4, Fig. 9L and M) suggest a marine influence of the dolomitizing fluids. The elemental composition of dolomite D4 is similar to the composition of dolomite D2 of the Lower Cangulo unit (D2, Fig. 10), with high Mg/Ca ratio and low Mn content. In this regard, the presence of domal laminated carbonates, cross bedded calcareous sandstones and highly bioturbated intervals *(?Ophiomorpha)* within the clastic dominated Upper Tumbalunda formation points to a return to marginal marine, tidal-influenced, mixed depositional environment comparable to the Lower Tumbalunda and Lower Cangulo units (Fig. 14G, H and 15F). The marginal marine interpretation of Upper Tumbalunda formation is in agreement with the equivalent deposits in Benguela area where well-exposed bivalve coquina facies filling tidal channels, and very clear *Ophiomorpha* and *Thallassinoides* traces have been identified. This final transgression terminated with the deposition of the Bambata evaporites, not preserved in the Cangulo palaeovalley but reported regionally (Gindre-Chanu et al., 2016). These evaporites were likely later mobilized, eroded and/or dissolved during Albian times, in addition to younger dissolution (Gindre-Chanu et al., 2015).

5.3. Regional implications for margin evolution

In the onshore Namibe and Benguela Basins the contact between the Upper Tumbalunda Fm. and the overlying evaporites of the Bambata Fm. is mostly gradational and transgressive in nature, with each successive bed and mixed tidal-sabkha parasequence onlapping and overstepping the palaeovalleys and associated interfluves, cumulating with an overstepping and widespread evaporite sheet deposited (Sharp et al., 2016). Progressive onlapping and overstepping transgressive valley filling parasequences are also commonly described for the age equivalent Grey Cuvo, Chela, and Gamba formations further north (Brownfield and Charpentier, 2006; Burwood, 1999; Karner et al., 2003; Van Eden, 1978.; Viera et al., 2015). Each parasequence has an increasingly evident marine/tidal signature, including in the Benguela (Dombe Grande) region (Fig. 16) a well-developed marine ichnofauna (*Thallassinoides, Ophiomorpha*) and locally exposed tidal channel filling bivalve and gastropod coquinas. In general, more obvious marginal marine tidal facies are evident in the Benguela pre-salt palaeovalley fill successions than in Namibe (Sharp et al., 2016), and these can be tied to an increasingly clear marine signal documented for the latest Chela/Cuvo in the northern Kwanza, Cabinda and Congo-Gabon region. Collectively these data could be interpreted to indicate a northerly marine connection/transgression direction for the latest pre-salt, which would be in keeping with the southerly propagation/opening direction suggested for the Kwanza-Campos, Namibe-Outer Santos conjugate rift arm based on regional offshore seismic tectono-stratigraphic mapping by Higgins et al. (2016). In all onshore areas of Angola an increasingly evaporitic facies association is evident in the uppermost pre-salt units towards the contact to the main Bambata Fm. evaporite. This includes locally well-developed halite pseudomorphs within tidal heterolithics, and interbedded cm scale cycles of evaporite, desiccated tidal flat muds and algal-fenestral carbonates (particularly well exposed in the Tumbalunda section). Ichnofaunas become sparse to absent in this uppermost section. In northern Namibe (Gaio and Tumbalunda regions) these uppermost pre-salt parasequences and main evaporite body backfill, onlap and overstep the palaeovalleys. A directly comparable situation is evident all along the Benguela to Kwanza basin margin outcrops (Fig. 16), leading Sharp et al. (2016) to conclude that, somewhat unusually, at least the initial phase of evaporitic deposition of the main Bambata/Loeme evaporite was transgressive in nature. Bambata/Loeme Fm. evaporites back-filling and overstepping palaeovalley features all along the Angolan margin, from Namibe to Kwanza, with very little evidence of coeval interbedded clastic deposition within the valleys is an important observation. This likely indicates an extreme phase of aridity and evaporation during the Middle Aptian, with effective palaeovalley fed clastic sediment supply shut off from the African craton. After the initial widespread Early Albian marine flooding event above the Bambata/Loeme evaporites (Binga/Gaio Mbr), clastic supply dramatically returns in the Middle Albian with thick red bed clastic successions of the Giraul and Dondo Fm's developed in the Namibe, Benguela and southern Kwanza basins.

Based on the present work, we cannot conclusively identify a unique regional or local mechanism that controlled the sea-level variations and T-R cycles recorded in the studied sedimentary succession. Additional detailed work in other localities of the margin would be required to get a better understanding of how the T-R cycles correlate from valley fill to valley fill from Namibe to Benguela and Kwanza. What we can say with some certainty however is that broadly age equivalent latest pre-salt sections in the Namibe, Benguela and southern Kwanza basins all display a similar overall backstepping onlapping valley filling and progressively overstepping mixed clastic-carbonate-evaporite sequence that passes gradationally upwards into the Bambata/Loeme evaporites (Fig. 16), and that these valley fill successions consist of a number of smaller scale transgressive-regressive cycles. A linked genetic relative sea level control thus appears obvious at the margin scale, although as to if base level changes were driven by eustatic versus regional tectonic/geodynamic controls at present remains unclear. The Aptian long term global eustatic sea level curve from Haq (2014) shows an overall high amplitude sea level fall trend, with several short-term cycles of sea level change. In the Atlantic the Early Aptian is associated with a sea level rise, whilst the Mid Aptian is associated with a significant relative sea level fall that is well documented in both the Atlantic and Tethyian realms, with some authors indicating a relative sea level fall of up to 120 m (Haq, 2014, Quirk and Rüpke, 2018). It is appealing to link the intra Tumbalunda unconformity or main South Atlantic evaporite phase to this major Mid Aptian sea level fall, as Quirk and Rüpke (2018) also concluded for the main evaporite phase. However, the as yet lack of precise dating of the studied onshore succession does not allow us to make this link with confidence.

The Cangulo study area is located at or just inboard of the Atlantic hinge of the necking domain (Fig. 2c), a zone which bounds the landward limit of post-rift thermal subsidence (Quirk and Rüpke, 2018). Faults observed at outcrop and on offshore seismic data offsetting sag units of the upper pre-salt units are also associated with folding of the evaporite and lower post-salt units up to the Lower Giraul Fm. Regionally, these faults and folds accommodate outer hinge zone tension at the transition between the outboard subsiding hyper-extended margin (outer basin, Fig. 16) and the stable inner marginal basin domain (Higgins et al., 2016). Regional pulsed or progressive seaward tilting of the African margin during this post-rift thermal relaxation (sag) phase could thus also be considered as a key driver on latest pre-salt sequence facies and thickness development, with pulsed basinwards rotation and regional tilting around the Atlantic hinge line driving the T-R cycles (Fig. 16). This mechanism could elegantly explain the regional basinwards fanning and expanding growth geometries observed within the latest Aptian pre-salt, evaporite and Albian post-salt successions all along the Angolan margin, resulting in a classic "steers head" like margin onlapping sag geometry as also suggested by Pindell et al. (2020). The hinge zone also controls the marked change in thickness of the sag, evaporite and immediate post salt successions from the thin inboard outcrops to the thick outboard/offshore sections (Fig. 16).

Placing the Cangulo palaeovalley study into a regional South Atlantic context, our onshore data unequivocally confirm the marginal marine evaporitic nature of the latest sag Pre-Salt successions. Given the outcrops studied are inboard of the main Atlantic Hinge or necking zone on relatively thick continental crust (Fig. 2), these new data have important implications for discussions of palaeobathymetry and water body composition (lacustrine vs marine) in the more offshore areas of the main Atlantic hinge immediately prior to the onset of deposition of the main South Atlantic evaporite (Karner et al., 2003; Sharp et al., 2016).

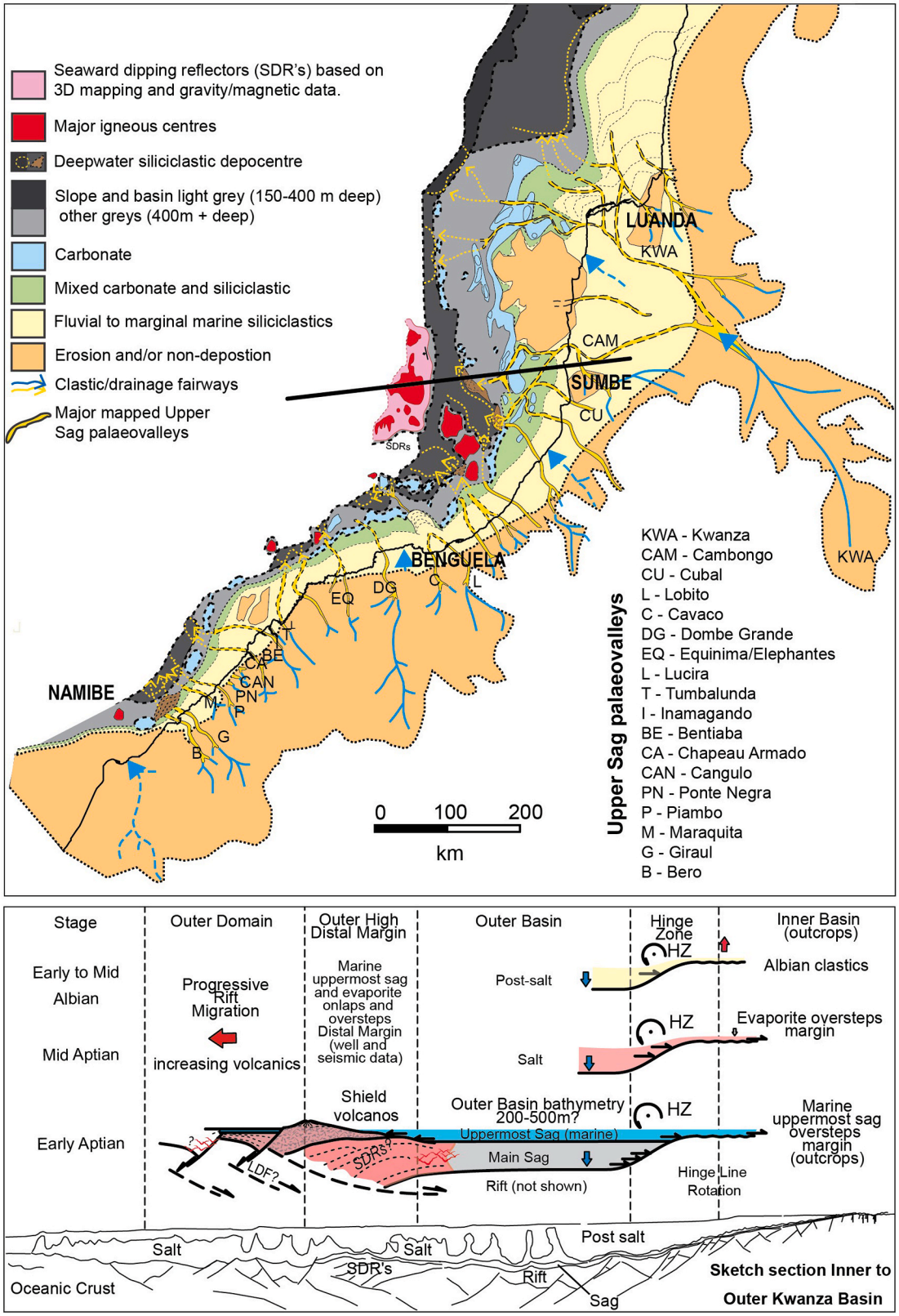

Fig. 16. Uppermost Sag Paleogeographic map (Aptian) – Angolan margin rotated clockwise to approximate 112 Ma position using Splates rotation model. Present day Angolan coastline outlined in black. Insert lower section showing interpreted main geodynamic events from Early Aptian to Early to Middle Albian. Section is based on regional seismic data across Kwanza Basin blocks 38, 22 and 7 tied to onshore sections. Thick black line on map shows location of the sketch section. Paleogeographic map shows interpreted depositional environments along the Angolan margin integrating outcrop, well and seismic data. Location of studied palaeovalleys indicated, included the Cangulo palaeovalley. SDR's – Seaward Dipping Reflectors. LDF – Landward Dipping Faults. HZ – Hinge Zone. Note the interpreted volcanic Outer High and SDR's in Kwanza Distal margin are not evident along strike in Benguela and Namibe, where the Distal Margin is more typically associated with interpreted exhumed mantle or crustal scale faulting. Uppermost Sag succession that forms the focus of this study is indicated in blue on lower sketch section, onlapping and overstepping both the Hinge Zone and Inner Basin (outcrops) and Distal Margin/Outer High.

The onshore marginal marine sections effectively act as a latest pre-salt relative sea level "datum" that can be projected outboard of the hinge line across the outer sag basins towards the volcanic outer highs (Fig. 16). Well data from age equivalent immediate pre-salt succession developed on the outer volcanic highs in the Kwanza Basin also confirm a marine signature, including the presence of marine red algae and echinoderm debris (Higgins et al., 2016; Sharp et al., 2016). Our new data confirm a latest pre-salt marine succession developed inboard of the main necking domain, and thus it appears unlikely that the South Atlantic Late Sag and evaporite in the outer basins was deposited in an underfilled Messinian-like silled basin significantly below regional sea level immediately prior to evaporation. An immediate Pre-salt marine datum in both the onshore and outer high areas would indicate that the intervening outer basins were marine in nature, with a palaeobathymetry and water depth of between 200 and 500 m based on seismic stratigraphic mapping and onlap relationships (Fig. 16). These are important conclusions with regard placing hard data constraints on the hotly debated nature of the depositional setting of the South Atlantic evaporites and latest sag deposits.

6. Conclusions

A 150 m-thick succession deposited in Cangulo palaeovalley exposed within the Namibe Basin is analysed in the present work. The studied succession belongs to upper sag deposits of the South Atlantic Pre-Salt succession, and is characterised by fluvial to marginal marine (tidal to sabkha) and non-marine sediments deposited during Aptian times in a well-developed Cretaceous palaeovalley. Regional mapping and comparisons indicate that Cangulo is not unique, with an age and facies equivalent network of pre-salt palaeovalley fill successions being evident along the SW Angolan margin from Namibe to Benguela and southern Kwanza (Fig. 16).

New data provide unambiguous evidence for a reinterpretation of the Pre-Salt carbonates of the Cangulo Fm., that were previously defined as a single depositional unit, as is summarised below.

The first early Aptian deposits in Cangulo palaeovalley (Lower Tumbalunda Fm.) corresponds to 2 transgressive-regressive cycles characterised by basal alluvial to fluvial coarse-grained deposits linked to systems flowing towards the west, transgressed by tidal marginal marine and tidal flat successions. The later transgressive package is characterised by the deposition of mixed siliciclastic, carbonate and evaporites associated with a maximum flooding event that reached very proximal parts of the palaeovalley. Early dolomitization of carbonates occurred, with marine fluids being the prevailing origin for this process ($\delta^{18}O$ between +2.04 and +3.27 ‰$_{VPDB}$ and $\delta^{13}C$ values between −1.11 and −0.22‰$_{VPDB}$).

After an abrupt regression and deposition of fluvial deposits, a third transgression resulted in the deposition of the Lower Cangulo unit in an intertidal-sabkha environment. This unit is interpreted to originally comprise an alternation of evaporite and carbonate interbeds, early dolomitized due to the circulation of mixed fluids. Dolostones located far from the basement walls of the palaeovalley point to a mixture of marine water and fluids derived from microbial sulphate reduction, organic matter oxidation and/or meteoric waters ($\delta^{18}O$ ranging from +0.64 to +3.64 ‰$_{VPDB}$ and $\delta^{13}C$ from −9.56 to −7.14‰$_{VPDB}$, and high Mg/Ca ratio). In areas near the basement, dolomitization was more influenced by meteoric fluids ($\delta^{18}O$ from 0.15 to 1.98 ‰$_{VPDB}$ and $\delta^{13}C$ from −16.41 to −11.86 ‰$_{VPDB}$, and low Mg/Ca ratio).

After deposition and dolomitization of the Lower Cangulo unit, a major regressive event with a shoreline migration of at least 1.5 km occurred, and meteoric fluids circulated and interacted with the previously deposited units. This event resulted in development of a large-scale erosive surface, the development of karstic systems and collapse breccias due to dissolution of evaporites. This major regressive event is stratigraphically dated as an intra Chela-Cuvo formation event, and is described here from the Namibe Basin for the first time.

The drop-off of the phreatic level during this regressive event caused onset of spring flows from basement highs and the development of the Upper Cangulo travertine complex, with geomorphology and geobody development closely linked to existing paleotopography. The $\delta^{18}O$ and $\delta^{13}C$ values of those deposits (−7.58 and −4.87 ‰$_{VPDB}$ and −15.83 and −7.64 ‰$_{VPDB}$ respectively) are consistent with precipitation from low/ambient temperature meteoric waters. Facies constituting travertine smooth slopes and pools (massive porous facies accompanied by dolomicrite-microsparite crusts) define a dynamic system with variation of the water flow regime pivoting between low-energy and rapid flows.

A final transgressive event flooded the Cangulo palaeovalley following deposition of the upper Cangulo unit travertine complex, resulting in deposition of tidally-influenced calcareous sandstones that onlap the travertine deposits. The elemental composition of partially dolomitized distal travertine beds (Ca and Mg content between $20.7{\cdot}10^4$ and $21.9{\cdot}10^4$ ppm and between $11.2{\cdot}10^4$ and $12.4{\cdot}10^4$ ppm respectively), suggest that mixed marine and meteoric waters were circulating at this time. The end of the transgression is marked by deposition of the Aptian aged evaporites (Bambata Fm.) representing the maximum transgressive stage, although they are not preserved in the Cangulo palaeovalley due to erosion and dissolution. Regional correlation indicates that the pre-salt Cangulo palaeovelly fill succession is not unique, but in fact represents a now well studied control section to compare to other West African palaeovalley fill successions evident in the onshore Namibe, Benguela and Southern Kwanza basins (Fig. 16).

The sedimentary and diagenetic reconstruction of the latest Pre-Salt succession of the onshore Namibe Basin demonstrates a periodic marine influence in the sedimentary record of onshore palaeovalleys, linked to at least four transgressive events. Thus, the latest Pre-Salt succession is not a simple transgressive event as interpreted previously, but rather there is a higher frequency transgressive-regressive story that controlled not only the depositional environments but also a complex succession of early diagenetic processes, including the deposition and partial removal of precursor evaporite bodies. Our new data have significant implications for the genesis of intra-late sag evaporitic successions know from the offshore basins, in addition to placing important constraints on the overall setting, bathymetry and transition from the sag to main evaporite period of deposition in the South Atlantic.

Declaration of competing interest

The authors declare that they have no known competing financial interests or personal relationships that could have appeared to influence the work reported in this paper.

Data availability

We have added our data as supplementary material

Acknowledgments

We thank Israel Cruz Orosa and Emilio Casciello for fruitful discussion during the development of the present study. Thanks to Equinor Angola and Rafael's camp staff for logistical support during field work, and all involved in the Equinor-Sonangol onshore field work collaboration program in the Namibe, Benguela and Kwanza basins between 2010 and 2014. Thank you to TGS for permission to use line drawing of seismic in Fig. 2. We thank associate editor Laura Tomassetti, Pierre-Alexandre Teboul and an anonymous reviewer who helped improve the quality of the manuscript. Carbon and oxygen isotopic analyses, and electron microprobe analyses were carried out at the Centre Científics i Tecnològics of the Universitat de Barcelona. XRD analyses were carried out in the laboratories of the Geoscience Barcelona (Geo3BCN–CSIC). This research is a contribution of the Group of Dynamics of the Lithosphere (GDL), Geosciences Barcelona (Geo3Bcn), Consejo Superior de Investigaciones Científicas (CSIC), Spain. The project work was

sponsored by Equinor (Norway), ALORBE Project (PIE–CSIC–202030E310), FEIBOB project (PGC2018-093903-B-C22) and ORRI Spanish project (PID2021-122467NB-C22). This research is within the framework of the Grups Consolidats de Recerca "Modelització Geodinàmica de la Litosfera" (2017SGR-847) and "Geologia Sedimentària" (SGR-Cat 2021 349).

Appendix A. Supplementary data

Supplementary data to this article can be found online at https://doi.org/10.1016/j.marpetgeo.2023.106153.

References

Andrews, J.E., 2006. Palaeoclimatic records from stable isotopes in riverine tufas: synthesis and review. Earth Sci. Rev. 75, 85–104. https://doi.org/10.1016/j.earscirev.2005.08.002.

Arenas, C., Casanova, J., Pardo, G., 1997. Stable-isotope characterization of the Miocene lacustrine systems of Los Monegros (Ebro Basin, Spain): palaeogeographic and palaeoclimatic implications. Palaeogeogr. Palaeoclimatol. Palaeoecol. 128, 133–155. https://doi.org/10.1016/S0031-0182(96)00052-1.

Baqués, V., Travé, A., Cantarero, I., 2013. Development of successive karstic systems within the baix penedès fault zone (onshore of the valencia trough, NW mediterranean). Geofluids 14, 75–94. https://doi.org/10.1111/gfl.12044.

Barnes, I., O'Neil, J.R., 1971. Calcium-magnesium carbonate solid solutions from Holocene conglomerate cements and travertines in the Coast Range of California. Geochem. Cosmochim. Acta 35, 699–718. https://doi.org/10.1016/0016-7037(71)90068-8.

Beglinger, S.E., Doust, H., Cloetingh, S., 2012. Relating petroleum system and play development to basin evolution: west African South Atlantic basins. Mar. Petrol. Geol. 30, 1–25. https://doi.org/10.1016/j.marpetgeo.2011.08.008.

Brownfield, M.E., Charpentier, R.R., 2006. Geology and Total Petroleum Systems of the West-Central Coastal Province (7203). USGS Bulletin, West Africa, p. 52. https://doi.org/10.3133/b2207B.

Budd, D.A., 1997. Cenozoic dolomites of carbonate islands: their attributes and origin. Earth Sci. Rev. 42, 1–47. https://doi.org/10.1016/S0012-8252(96)00051-7.

Burwood, R., 1999. Angola: Source Rock Control for Lower Congo Coastal and Kwanza Basin Petroleum Systems. Geological Society Special Publication, pp. 181–194. https://doi.org/10.1144/GSL.SP.1999.153.01.12.

Bustillo, M.A., Armenteros, I., Huerta, P., 2017. Dolomitization, gypsum calcitization and silicification in carbonate–evaporite shallow lacustrine deposits. Sedimentology 64, 1147–1172. https://doi.org/10.1111/sed.12345.

Cameron, N., Bate, R., Clure, V., Benton, J., 1999. Oil and Gas Habitats of the South Atlantic: Introduction, vol. 153. Geological Society, London, Special Publications, pp. 1–9. https://doi.org/10.1144/gsl.sp.1999.153.01.01.

Capezzuoli, E., Gandin, A., Pedley, M., 2014. Decoding tufa and travertine (fresh water carbonates) in the sedimentary record: the state of the art. Sedimentology 61, 1–21. https://doi.org/10.1111/sed.12075.

Chafetz, H.S., Folk, R.L., 1984. Travertines; depositional morphology and the bacterially constructed constituents. J. Sediment. Res. 54, 289–316. https://doi.org/10.1306/212f8404-2b24-11d7-8648000102c1865d.

Chumakov, N.M., 1995. The problem of the warm biosphere. Stratigr. Geol. Correl. 3, 205–215. URI: https://oceanrep.geomar.de/id/eprint/52392.

Claypool, G.E., Holser, W.T., Kaplan, I.R., Sakai, H., Zak, I., 1980. The age curves of sulfur and oxygen isotopes in marine sulfate and their mutual interpretation. Chem. Geol. 28, 199–260. https://doi.org/10.1016/0009-2541(80)90047-9.

Dalrymple, R.W., Choi, K., 2007. Morphologic and facies trends through the fluvial–marine transition in tide-dominated depositional systems: a schematic framework for environmental and sequence-stratigraphic interpretation. Earth Sci. Rev. 81, 135–174. https://doi.org/10.1016/j.earscirev.2006.10.002.

Daniels, S.E., Tucker, M.E., Mawson, M.J., Holdsworth, R.E., Long, J.J., Gluyas, J.G., Jones, R.R., 2020. Nature and origin of collapse breccias in the Zechstein of NE England: local observations with cross-border petroleum exploration and production significance, across the North Sea. Geological Society, London, Special Publications 494, SP494. https://doi.org/10.1144/sp494-2019-140, 2019-2140.

Davis, R.A., 2012. Tidal signatures and their preservation potential in stratigraphic sequences. In: Davis Jr., R.A., Dalrymple, R.W. (Eds.), Principles of Tidal Sedimentology. Springer Netherlands, Dordrecht, pp. 35–55. https://doi.org/10.1007/978-94-007-0123-6_3.

de Carvalho, G.S., 1961. Geologia do deserto de Moçâmedes. (Angola) Uma contribuição para o conhecimento dos problemas da orla sedimentar de Moçâmedes, Lisbon (Portugal).

De Carvalho, H., Tassinari, C., Alves, P.H., Guimarães, F., Simões, M.C., 2000. Geochronological review of the Precambrian in western Angola: links with Brazil. J. Afr. Earth Sci. 31, 383–402. https://doi.org/10.1016/S0899-5362(00)00095-6.

Della Porta, G., 2015. Carbonate build-ups in lacustrine, hydrothermal and fluvial settings: comparing depositional geometry, fabric types and geochemical signature. Geological Society, London, Special Publications 418, 17–68. https://doi.org/10.1144/sp418.4.

Della Porta, G., Croci, A., Marini, M., Kele, S., 2017. Depositional architecture, facies character and geochemical signature of the Tivoli travertines (Pleistocene, Acque Albule basin, Central Italy). Riv. Ital. Paleontol. Stratigr. 123, 487–540. https://doi.org/10.13130/2039-4942/9148.

Dietrich, P., Griffis, N.P., Le Heron, D.P., Montañez, I.P., Kettler, C., Robin, C., Guillocheau, F., 2021. Fjord network in Namibia: a snapshot into the dynamics of the late Paleozoic glaciation. Geology 49 (12), 1521–1526, 2021.

Equinor, 2011. Tectono-stratigraphic Evolution of an Oblique Rifted Margin. Namibe Basin Case Study, Angola (Unpublished internal company report).

Erthal, M.M., Capezzuoli, E., Mancini, A., Claes, H., Soete, J., Swennen, R., 2017. Shrub morpho-types as indicator for the water flow energy - tivoli travertine case (Central Italy). Sediment. Geol. 347, 79–99. https://doi.org/10.1016/j.sedgeo.2016.11.008.

Ferreri, V., Weissert, H., D'Argenio, B., Buonocunto, F.P., 1997. Carbon isotope stratigraphy: a tool for basin to carbonate platform correlation. Terra. Nova 9, 57–61. https://doi.org/10.1111/j.1365-3121.1997.tb00002.x.

Fiordalisi, E., Marchegiano, M., John, C.M., Oxtoby, N., Rochelle-Bates, N., do Couto Pereira, G., Machado, V.A.G., Dixon, R., Sharp, I., Schröder, S., 2021. Late cretaceous volcanism and fluid circulation in the South Atlantic: insights from continental carbonates in the onshore Namibe Basin (Angola). Mar. Petrol. Geol. 134, 105351 https://doi.org/10.1016/j.marpetgeo.2021.105351.

Folk, R.L., 1994. Interaction between bacteria, nannobacteria, and mineral precipitation in hot springs of central Italy. Géogr. Phys. Quaternaire 48, 233–246. https://doi.org/10.7202/033005ar.

Folk, R.L., Land, L.S., 1975. Mg/Ca ratio and salinity: two controls over crystallization of Dolomite1. AAPG (Am. Assoc. Pet. Geol.) Bull. 59, 60–68. https://doi.org/10.1306/83d91c0e-16c7-11d7-8645000102c1865d.

Friedman, G.M., 1997. Dissolution-collapse breccias and paleokarst resulting from dissolution of evaporite rocks, especially sulfates. Carbonates Evaporites 12, 53–63. https://doi.org/10.1007/BF03175802.

Friedman, I., O'Neil, J.R., 1977. Compilation of stable isotope fractionation factors of geochemical interest. In: Fleischer, M. (Ed.), Data of Geochemistry, sixth ed. United States Goverment Printing Office, Washington (U.S), pp. 1–112. https://doi.org/10.3133/pp440KK.

Gandin, A., Capezzuoli, E., 2008. Travertine versus calcareous tufa: distinctive petrological features and stable isotope signatures. Italian Journal of Quaternary Sciences 21, 125–136.

Gandin, A., Capezzuoli, E., 2014. Travertine: distinctive depositional fabrics of carbonates from thermal spring systems. Sedimentology 61, 264–290. https://doi.org/10.1111/sed.12087.

Geske, A., Zorlu, J., Richter, D.K., Buhl, D., Niedermayr, A., Immenhauser, A., 2012. Impact of diagenesis and low grade metamorphosis on isotope (δ26Mg, δ13C, δ18O and 87Sr/86Sr) and elemental (Ca, Mg, Mn, Fe and Sr) signatures of Triassic sabkha dolomites. Chem. Geol. 332–333, 45–64. https://doi.org/10.1016/j.chemgeo.2012.09.014.

Gindre-Chanu, L., Perri, E., Sharp, I., Peacock, D.C.P., Swart, R., Poulsen, R., Ferreira, H., Machado, V., 2016. Origin and diagenetic evolution of gypsum and microbialitic carbonates in the Late Sag of the Namibe Basin (SW Angola). Sediment. Geol. 342, 133–153. https://doi.org/10.1016/j.sedgeo.2016.06.015.

Gindre-Chanu, L., Warren, J.K., Puigdefabregas, C., Sharp, I.R., Peacock, D.C.P., Swart, R., Poulsen, R., Ferreira, H., Henrique, L., 2015. Diagenetic evolution of aptian evaporites in the Namibe Basin (south-west Angola). Sedimentology 62, 204–233. https://doi.org/10.1111/sed.12146.

Globig, J., Fernàndez, M., Torne, M., Vergés, J., Robert, A., Faccenna, C., 2016. New insights into the crust and lithospheric mantle structure of Africa from elevation, geoid, and thermal analysis. J. Geophys. Res. Solid Earth 121, 5389–5424. https://doi.org/10.1002/2016JB012972.

Guiraud, M., Buta-Neto, A., Quesne, D., 2010. Segmentation and differential post-rift uplift at the Angola margin as recorded by the transform-rifted Benguela and oblique-to-orthogonal-rifted Kwanza basins. Mar. Petrol. Geol. 27, 1040–1068. https://doi.org/10.1016/j.marpetgeo.2010.01.01.

Guo, L., Riding, R., 1998. Hot-spring travertine facies and sequences, Late Pleistocene. Rapolano Terme, Italy. Sedimentology 45, 163–180. https://doi.org/10.1046/j.1365-3091.1998.00141.x.

Haq, B.U., 2014. Cretaceous eustasy revisited. Global Planet. Change 113, 44–58.

Hay, W.W., Floegel, S., 2012. New thoughts about the Cretaceous climate and oceans. Earth Sci. Rev. 115, 262–272. https://doi.org/10.1016/j.earscirev.2012.09.008.

Hayes, M.J., Boles, J.R., 1993. Evidence for meteoric recharge in the San Joaquin basin, California provided by isotope and trace element chemistry of calcite. Mar. Petrol. Geol. 10, 135–144. https://doi.org/10.1016/0264-8172(93)90018-N.

Heine, C., Zoethout, J., Müller, R.D., 2013. Kinematics of the South Atlantic rift. Solid Earth 4, 215–253. https://doi.org/10.5194/se-4-215-2013.

Higgins, S., Messager, G., Sharp, I., Scott, M., Freitag, U., Groger, h., 2016. Tectono-Stratigraphic Evolution and Variability of the Offshore Central South Atlantic Basins - Implications for Margin Evolution Models, Rifts III: Catching the Wave. Geological Society of London, London, UK.

Isbell, J.L., Cole, D.I., Catuneanu, O., 2008. Carboniferous-Permian glaciation in the main Karoo Basin, South Africa: stratigraphy, depositional controls, and glacial dynamics. In: Fielding, C.R., Frank, T.D., Isbell, J.L. (Eds.), Resolving the Late Paleozoic Ice Age in Time and Space, vol. 441. Geological Society of America Special Paper, pp. 71–82. https://doi.org/10.1130/2008.2441(05.

Jerram, D.A., Sharp, I.R., Torsvik, T.H., Poulsen, R., Watton, T., Freitag, U., Halton, A., Sherlock, S.C., Malley, J.A.S., Finley, A., Roberge, J., Swart, R., Puigdefabregas, C., Ferreira, C.H., Machado, V., 2019. Volcanic constraints on the unzipping of Africa from South America: insights from new geochronological controls along the Angola margin. Tectonophysics 760, 252–266. https://doi.org/10.1016/j.tecto.2018.07.027.

Karner, G.D., Driscoll, N.W., Barker, D.H.N., 2003. Syn-rift regional subsidence across the West African continental margin: the role of lower plate ductile extension.

Geological Society, London, Special Publications 207, 105–129. https://doi.org/10.1144/gsl.sp.2003.207.6.
Kervin, R.J., Woods, A.D., 2012. Origin and evolution of palaeokarst within the lower ordovician (ibexian) goodwin formation (pogonip Group). J. Palaeogeogr. 1, 57–69. https://doi.org/10.3724/SP.J.1261.2012.00006.
Kitano, Y., 1963. Geochemistry of calcareous deposits found in hot springs. J. Earth Sci. Nagoya Univ. 11, 68–100.
Lasemi, Y., Jahani, D., Amin-Rasouli, H., Lasemi, Z., 2012. Ancient carbonate tidalites. In: Davis Jr., R.A., Dalrymple, R.W. (Eds.), Principles of Tidal Sedimentology. Springer Netherlands, Dordrecht, pp. 567–607. https://doi.org/10.1007/978-94-007-0123-6_21.
Li, M., Lin, X., Tian, J., Peng, S., Xu, L., Su, L., 2019. Study on variously dolomitized reservoir reef at platform margin of Changxing Formation in northeastern Sichuan Basin, southwestern China. Carbonates Evaporites 34, 609–622. https://doi.org/10.1007/s13146-018-0429-y.
Lohmann, K.C., 1988. In: James, N.P., Choquette, P.W. (Eds.), Geochemical Patterns of Meteoric Diagenetic Systems and Their Application to Studies of Paleokarst, Paleokarst. Springer, New York (USA), pp. 58–80. https://doi.org/10.1007/978-1-4612-3748-8_3.
Long, D.T., Fegan, N.E., McKee, J.D., Lyons, W.B., Hines, M.E., Macumber, P.G., 1992. Formation of alunite, jarosite and hydrous iron oxides in a hypersaline system: lake Tyrrell, Victoria, Australia. Chem. Geol. 96, 183–202. https://doi.org/10.1016/0009-2541(92)90128-R.
Luo, L., Capezzuoli, E., Vaselli, O., Wen, H., Lazzaroni, M., Lu, Z., Meloni, F., Kele, S., 2021a. Factors governing travertine deposition in fluvial systems: the Bagni San Filippo (central Italy) case study. Sediment. Geol. 426, 106023 https://doi.org/10.1016/j.sedgeo.2021.106023.
Luo, L., Wen, H., Capezzuoli, E., 2021b. Travertine deposition and diagenesis in Ca-deficiency perched hot spring systems: a case from Shihuadong, Tengchong, China. Sediment. Geol. 414, 105827 https://doi.org/10.1016/j.sedgeo.2020.105827.
Marsh, J.S., Swart, R., 2018. The Bero volcanic complex: extension of the paraná-etendeka igneous province into SW Angola. J. Volcanol. Geoth. Res. 355, 21–31. https://doi.org/10.1016/j.jvolgeores.2016.10.011.
Marton, L.G., Tari, G.C., Lehmann, C.T., 2000. Evolution of the Angolan passive margin, West Africa, with emphasis on post-salt structural styles. In: Mohriak, W.U., Talwani, M. (Eds.), Atlantic Rifts and Continental Margins. American Geophysical Union, Washington, DC, pp. 129–149.
Marzoli, A., Melluso, L., Morra, V., Renne, P.R., Sgrosso, I., D'Antonio, M., Duarte Morais, L., Morais, E.A.A., Ricci, G., 1999. Geochronology and petrology of Cretaceous basaltic magmatism in the Kwanza basin (western Angola), and relationships with the Paranà-Etendeka continental flood basalt province. J. Geodyn. 28, 341–356. https://doi.org/10.1016/S0264-3707(99)00014-9.
Masse, P., Laurent, O., 2016. Geological exploration of Angola from Sumbe to Namibe: a review at the frontier between geology, natural resources and the history of geology. Compt. Rendus Geosci. 348, 80–88. https://doi.org/10.1016/j.crte.2015.09.007.
Matysik, M., 2016. Facies types and depositional environments of a morphologically diverse carbonate platform: a case study from the Muschelkalk (middle Triassic) of Upper Silesia, Southern Poland. Ann. Soc. Geol. Pol. 86, 119–164. https://doi.org/10.14241/asgp.2016.013.
Mazzullo, S.J., 2000. Organogenic dolomitization in peritidal to deep-sea sediments. J. Sediment. Res. 70, 10–23. https://doi.org/10.1306/2dc408f9-0e47-11d7-8643000102c1865d.
McCourt, S., Armstrong, R.A., Jelsma, H., Mapeo, R.B.M., 2013. New U–Pb SHRIMP ages from the lubango region, SW Angola: insights into the palaeoproterozoic evolution of the Angolan Shield, southern Congo Craton, Africa. J. Geol. Soc. 170, 353–363. https://doi.org/10.1144/jgs2012-059.
Mercedes-Martín, R., Salas, R., Arenas, C., 2014. Microbial-dominated carbonate platforms during the Ladinian rifting: sequence stratigraphy and evolution of accommodation in a fault-controlled setting (Catalan Coastal Ranges, NE Spain). Basin Res. 26, 269–296. https://doi.org/10.1111/bre.12026.
Moore, C.H., 2001. Carbonate Reservoirs: Porosity Evolution and Diagenesis in a Sequence Stratigraphic Framework. Elsevier Science Limited.
Moore, C.H., Wade, W.J., 2013. Carbonate Reservoirs: Porosity and Diagenesis in a Sequence Stratigraphic Framework. Elsevier Science.
Moulin, M., Aslanian, D., Rabineau, M., Patriat, M., Matias, L., 2013. Kinematic keys of the santos–namibe basins. Geological Society, London, Special Publications 369, 91–107. https://doi.org/10.1144/sp369.3.
Özkul, M., Kele, S., Gökgoz, A., Shen, C.C., Baykara, M.O., Fórizs, I., Németh, T., Chang, Y.-W., Alçiçek, M.C., 2013. Comparison of the Quaternary travertine sites in the Denisli extensional basin based on their deposition and geochemical data. Sediment. Geol. 294, 179–204. https://doi.org/10.1016/j.sedgeo.2013.05.018.
Özkul, M., Varol, B., Alçiçek, M.C., 2002. Depositional environments and petrography of Denizli travertines. Bulletin of the Mineral Research and Exploration 125, 13–29.
Pentecost, A., Viles, H., 1994. A review and reassessment of travertine classification. Géogr. Phys. Quaternaire 48, 305–314. https://doi.org/10.7202/033011aradresse copiéeune erreur s'est produite.
Pérez-Díaz, L., Eagles, G., 2014. Constraining South Atlantic growth with seafloor spreading data. Tectonics 33, 1848–1873. https://doi.org/10.1002/2014TC003644.
Pindell, J., Graham, R., Horn, B.W., 2020. Role of outer marginal collapse on salt deposition in the eastern Gulf of Mexico, Campos and Santos basins. Geological Society, London, Special Publications 476 (1), 317–331.
Preto, N., Breda, A., Dal Corso, J., Spötl, C., Zorzi, F., Frisia, S., 2015. Primary dolomite in the late triassic travenanzes formation, dolomites, northern Italy: facies control and possible bacterial influence. Sedimentology 62, 697–716. https://doi.org/10.1111/sed.12157.
Quesne, D., Buta-Neto, A., Benard, D., Guiraud, M., 2009. 2009. Distribution of albian clastic deposits in the Benguela basin (Angola): evidence of a Benguela palaeocurrent? Bull. Soc. Geol. Fr. 180 (2), 117–129. https://doi.org/10.2113/gssgfbull.180.2.117.
Quirk, D.G., Rüpke, L.H., 2018. Melt-induced buoyancy may explain the elevated rift-rapid sag paradox during breakup of continental plates. Sci. Rep. 8 (1), 1–13.
Rainey, D.K., Jones, B., 2009. Abiotic versus biotic controls on the development of the Fairmont Hot Springs carbonate deposit, British Columbia, Canada. Sedimentology 56, 1832–1857. https://doi.org/10.1111/j.1365-3091.2009.01059.x.
Rankey, E.C., Berkeley, A., 2012. Holocene carbonate tidal flats. In: Davis Jr., R.A., Dalrymple, R.W. (Eds.), Principles of Tidal Sedimentology. Springer Netherlands, Dordrecht, pp. 507–535. https://doi.org/10.1007/978-94-007-0123-6_19.
Rasband, W.S., 1997. ImageJ: Image Processing and Analysis in Java. National Institutes of Health, Bethesda, Maryland, USA.
Renaut, R.W., Jones, B., 1997. Controls on aragonite and calcite precipitation in hot spring travertines at Chemurkeu, Lake Bogoria, Kenya. Can. J. Earth Sci. 34, 801–818. https://doi.org/10.1139/e17-066.
Renaut, R.W., Owen, R.B., Jones, B., Tiercelin, J.-J., Tarits, C., Ego, J.K., Konhauser, K. O., 2013. Impact of lake-level changes on the formation of thermogene travertine in continental rifts: evidence from Lake Bogoria, Kenya Rift Valley. Sedimentology 60, 428–468. https://doi.org/10.1111/j.1365-3091.2012.01347.x.
Reston, T.J., 2010. The opening of the central segment of the South Atlantic: symmetry and the extension discrepancy. Petrol. Geosci. 16, 199–206. https://doi.org/10.1144/1354-079309-907.
Rochelle-Bates, N., Roberts, N.M.W., Sharp, I., Freitag, U., Verwer, K., Halton, A., Fiordalisi, E., van Dongen, B.E., Swart, R., Ferreira, C.H., Dixon, R., Schröder, S., 2021. 2020. Geochronology of volcanically associated hydrocarbon charge in the pre-salt carbonates of the Namibe Basin, Angola. Geology 49 (3), 335–340. https://doi.org/10.1130/g48019.1.
Sabato-Ceraldi, T., Green, D., 2016. Evolution of the South Atlantic lacustrine deposits in response to Early Cretaceous rifting, subsidence and lake hydrology. Geological Society, London, Special Publications 438, 77–98. https://doi.org/10.1144/SP438.10.
Salardon, R., Carpentier, C., Bellahsen, N., Pironon, J., France-Lanord, C., 2017. Interactions between tectonics and fluid circulations in an inverted hyper-extended basin: example of mesozoic carbonate rocks of the western North Pyrenean Zone (Chaînons Béarnais, France). Mar. Petrol. Geol. 80, 563–586. https://doi.org/10.1016/j.marpetgeo.2016.11.018.
Salvany, J.M., García-Veigas, J., Ortí, F., 2007. Glauberite–halite association of the zaragoza gypsum formation (lower Miocene, ebro basin, NE Spain). Sedimentology 54, 443–467. https://doi.org/10.1111/j.1365-3091.2006.00844.x.
Schettino, A., Scotese, C.R., 2005. Apparent polar wander paths for the major continents (200 Ma to the present day): a palaeomagnetic reference frame for global plate tectonic reconstructions. Geophys. J. Int. 163, 727–759. https://doi.org/10.1111/j.1365-246X.2005.02638.x.
Scholle, P.A., Stemmerik, L., Ulmer-Scholle, D., Liegro, G.D., Henk, F.H., 1993. Palaeokarst-influenced depositional and diagenetic patterns in Upper Permian carbonates and evaporites, Karstryggen area, central East Greenland. Sedimentology 40, 895–918. https://doi.org/10.1111/j.1365-3091.1993.tb01368.x.
Schröder, S., Ibekwe, A., Saunders, M., Dixon, R., Fisher, A., 2016. Algal–microbial carbonates of the Namibe Basin (Albian, Angola): implications for microbial carbonate mound development in the South Atlantic. Petrol. Geosci. 22, 71. https://doi.org/10.1144/petgeo2014-083.
Sharp, I., Higgins, S., Messager, G., Swart, R., Marsh, J.S., Gindre-Chanu, L., Puigdefàbregas, C., Verwer, K., Ferreira, H., Snidero, M., Machado, V., Holtar, E., Dongala, M., Jerram, D., Blanc, E., Groger, H., Scott, M., Freitag, U., Lapponi, F., Vergés, J., Hunt, D., Zeller, M., Martín-Martín, J.D., Moragas, M., Cruz, I., Baqués, V., Casciello, E., Wennberg, O.P., Warren, J.K., 2016. Tectono-Stratigraphic Evolution of the Onshore Namibe-Benguela-Kwanza Basins, Angola - Implications for Margin Evolution Models, Rift III: Catching the Wave. Geological Society of London, London, UK.
Sharp, I., Verwer, K., Ferreira, C.H., Snidero, M., Machado, V., Holtar, E., Swart, R., Marsh, J., Gindre-Chanu, L., Puigdefàbregas, C., Fejerskov, M., 2012. Pre- and Post-Salt Non-marine Carbonates of the Namibe Basin, Angola, AAPG Annual Convention and Exhibition. American Association of Petroleum Geologists, Long Beach, California (USA).
Shinn, E.A., Scholle, P.A., Bebout, D.G., Moore, C.H., 1983. Tidal Flat Environment, in: Carbonate Depositional Environments, vol. 33. American Association of Petroleum Geologists. https://doi.org/10.1306/m33429c8.
Strganac, C., Salminen, J., Jacobs, L.L., Polcyn, M.J., Ferguson, K.M., Mateus, O., Schulp, A.S., Morais, M.L., Tavares, T.d.S., Gonçalves, A.O., 2014. Carbon isotope stratigraphy, magnetostratigraphy, and 40Ar/39Ar age of the cretaceous South Atlantic coast, Namibe Basin, Angola. J. Afr. Earth Sci. 99, 452–462. https://doi.org/10.1016/j.jafrearsci.2014.03.003.
Swart, R., Puigdefàbregas, C., Holtar, E., 2016. The geology of the Namibe Basin. In: London, G.S.o. (Ed.), Rifts III: Catching the Waves. Geological Society of London, London (United Kingdom).
Swennen, R., Viaene, W., Cornelissen, C., 1990. Petrography and geochemistry of the Belle Roche breccia (lower Visean, Belgium): evidence for brecciation by evaporite dissolution. Sedimentology 37, 859–878. https://doi.org/10.1111/j.1365-3091.1990.tb01830.x.
Szatmari, P., Milani, E.J., 2016. Tectonic control of the oil-rich large igneous-carbonate-salt province of the South Atlantic rift. Mar. Petrol. Geol. 77, 567–596. https://doi.org/10.1016/j.marpetgeo.2016.06.004.
Teboul, P.-A., Durlet, C., Girard, J.-P., Dubois, L., San Miguel, G., Virgone, A., Gaucher, E.C., Camoin, G., 2019. Diversity and origin of quartz cements in

continental carbonates: example from the Lower Cretaceous rift deposits of the South Atlantic margin. Appl. Geochem. 100, 22–41. https://doi.org/10.1016/j.apgeochem.2018.10.019.

Torsvik, T.H., Rousse, S., Labails, C., Smethurst, M.A., 2009. A new scheme for the opening of the South Atlantic Ocean and the dissection of an Aptian salt basin. Geophys. J. Int. 177, 1315–1333. https://doi.org/10.1111/j.1365-246X.2009.04137.x.

Travé, A., Rodríguez-Morillas, N., Baqués, V., Playà, E., Casas, L., Cantarero, I., Martín-Martín, J.D., Gómez-Rivas, E., Moragas, M., Cruset, D., 2021. Origin of the coloured karst fills in the neogene extensional system of NE iberia (Spain). Minerals 11, 1382. https://doi.org/10.3390/min11121382.

Tucker, M.E., 1991. Sequence stratigraphy of carbonate-evaporite basins: models and application to the upper permian (zechstein) of northeast england and adjoining north sea. J. Geol. Soc. 148, 1019–1036. https://doi.org/10.1144/gsjgs.148.6.1019.

Van Eden, J.G., 1978. Stratiform copper and zinc mineralization in the Cretaceous of Angola. Econ. Geol. 73, 1154–1161. https://doi.org/10.2113/gsecongeo.73.6.1154.

Veizer, J., Ala, D., Azmy, K., Bruckschen, P., Buhl, D., Bruhn, F., Carden, G.A.F., Diener, A., Ebneth, S., Godderis, Y., Jasper, T., Korte, C., Pawellek, F., Podlaha, O.G., Strauss, H., 1999. 87Sr/86Sr, δ13C and δ18O evolution of Phanerozoic seawater. Chem. Geol. 161, 59–88. https://doi.org/10.1016/S0009-2541(99)00081-9.

Viera, A.F., Pereria, D.M., Ragazzi, M.D., Tudisca, E., Giacomone, G., 2015. Environmental setting of the Chela Formation in the onshore of Cabinda province, republic of Angola. SEG Global Meeting Abstracts 440, 440.

Warren, J.K., 2016. Evaporites: A Geological Compendium, second ed. ed. Springer, ISBN 3540323449. 9783540323440.

Wen, Z., Jiang, S., Song, C., Wang, Z., He, Z., 2019. Basin evolution, configuration styles, and hydrocarbon accumulation of the South Atlantic conjugate margins. Energy Explor. Exploit. 37, 992–1008. https://doi.org/10.1177/0144598719840751.

Wright, P., 1990. Carbonate depositional systems I: marine shallow-water and lacustrine carbonates (peritidal carbonates). In: Tucker, M., Wright, P. (Eds.), Carbonate Sedimentology. Blackwell Science Ltd., Oxford (U.K), pp. 101–227. https://doi.org/10.1002/9781444314175.ch4.

Zeng, L., Ruge, D.B., Berger, G., Heck, K., Hölzl, S., Reimer, A., Jung, D., Arp, G., 2021. Sedimentological and carbonate isotope signatures to identify fluvial processes and catchment changes in a supposed impact ejecta-dammed lake (Miocene, Germany). Sedimentology 68, 2965–2995. https://doi.org/10.1111/sed.12888.